Improved calculation of the primordial gravitational wave spectrum in the standard model

Yuki Watanabe*

Department of Physics, University of Texas, Austin, Texas 78712, USA

Eiichiro Komatsu

Department of Astronomy, University of Texas, Austin, Texas 78712, USA

We show that the energy density spectrum of the primordial gravitational waves has characteristic features due to the successive changes in the relativistic degrees of freedom during the radiation era. These changes make the evolution of radiation energy density deviate from the conventional adiabatic evolution, $\rho_r \propto a^{-4}$, and thus cause the expansion rate of the universe to change suddenly at each transition which, in turn, modifies the spectrum of primordial gravitational waves. We take into account all the particles in the standard model of elementary particles. In addition, free-streaming of neutrinos damps the amplitude of gravitational waves, leaving characteristic features in the energy density spectrum. Our calculations are solely based on the standard model of cosmology and particle physics, and therefore these features must exist. Our calculations significantly improve the previous ones which ignored these effects and predicted a smooth, featureless spectrum.

I. INTRODUCTION

Detection of the stochastic background of primordial gravitational waves has profound implications for the physics of the early universe and the high energy physics that is not accessible by particle accelerators [1–13]. The basic reason why relic gravitational waves carry information about the very early universe is that particles which decoupled from the primordial plasma at a certain time, $t \sim t_{\rm dec}$, when the universe had a temperature of $T \sim T_{\rm dec}$, memorize the physical state of the universe at and below $T_{\rm dec}$. Since gravitons decoupled below the Plank energy scale, the relic gravitons memorize all the expansion history of the universe after they decoupled and thus would probe deeper into the very early universe. Gravitational waves act therefore as the *time machine* that allows us to see through the entire history of the universe. Another example of relic species is the cosmic microwave background (CMB) photons, which decoupled from matter at $T \sim 0.3$ eV and can trace the physical state of the universe back to 0.3 eV. On the other hand, the primordial gravitational waves carry information on the state of the much earlier universe than the CMB photons do.

The purpose of this paper is to study the evolution of primordial gravitational waves through changes in the physical conditions in the universe within the standard model (SM) of elementary particles and beyond. For instance, the quark gluon plasma (QGP) phase to hadron gas phase transition causes a sharp feature in the gravitational wave spectrum. The change of the number of relativistic degrees of freedom affects the Hubble rate by reducing the growth rate of the Hubble radius during the transition. Thus, the rate at which modes re-enter the horizon is

changed during the transition and a step in the spectrum appears at frequencies on the order of the Hubble rate at the transition. For the QGP phase transition this frequency is $\sim 10^{-7}$ Hz today and the correction is about 30% [14]. Other large drops in the number of relativistic degrees of freedom occur at electron-positron annihilation and possibly at the supersymmetry (SUSY) breaking. Since the gravitational wave spectrum is sensitive to the number of relativistic degrees of freedom, one can search for evidence of supersymmetry in the very beginning of the universe by looking at the relevant frequency region ($\sim 10^{-3}$ Hz). For energy scales lower than neutrino decoupling (~ 2 MeV [15]) we shall also account for the damping effect from neutrino free-streaming [16–18]. We show that a combination of these two effects gives rise to a highly nontrivial shape of the gravitational wave spectrum.

The primordial gravitational wave spectrum will also provide us with information about inflation. The energy scale of inflation is directly related to the amplitude of the spectrum. The modes which re-entered the horizon during the radiation-dominated epoch show a nearly scale-invariant spectrum if we do not consider the change of the effective number of degrees of freedom. Typically the amplitude of the spectrum is of order 10^{-15} for 10^{16} GeV inflation energy scale in such a frequency region. Inflation ends when the inflaton decays into radiation and reheats the universe [19–21]. The energy scale of reheating could be seen from the highest frequency end ($\sim k_{\rm rh}$) of a nearly scale-invariant energy density spectrum of the primordial gravitational waves. The lowest frequency mode observable today corresponds to the horizon size today, and the interval between the lowest frequency and $k_{\rm rh}$ would give the number of *e*-holdings, which tells us the duration of inflation between the end of inflation and the time at which fluctuations having the wavelength of the current horizon

---

*Electronic address: yuki@astro.as.utexas.edu

size left the horizon during inflation. The slope of the spectrum provides the power-law index of the tensor perturbation, n_T [10,12]. $n_T = 0$ corresponds to a scale-invariant power spectrum from de Sitter inflation. In a large class of inflationary models $|n_T|$ is not zero but much smaller than unity, and its determination constrains the inflationary models. As the effect of n_T has been investigated by many authors, e.g. [10–12,22,23], and is easy to include, we shall assume de Sitter inflation ($n_T = 0$) throughout this paper. Our result is general and easily applicable to any kind of models which produce primordial tensor perturbations. (e.g. ekpyrotic models [24]).

The primordial gravitational waves not only test and probe the physics of inflation and reheating, but also can provide the tomography of the SM of particle physics and models beyond. The study of its spectrum enables us to probe the very early universe in a truly transparent way. The goal of this paper is to show how the constituents in the early and very early universe would affect the primordial gravitational wave spectrum, which is observable in principle and may be observable in the future by the next generation observational projects, such as the Big Bang Observer (BBO) proposed to NASA [25] and the DECIGO proposed in Japan [26]. We present a new, rigorous computation of the primordial gravitational wave spectrum from de Sitter inflation with the SM of particle physics. It is easy to extend our results to non-de Sitter (e.g., slow-roll) inflation models.

The outline of this paper is as follows. In Sec. II, basics about the primordial gravitational waves from inflation are reviewed. In Sec. III, a crucial quantity during radiation domination, the effective relativistic degrees of freedom, g_*, is introduced and related to the primordial gravitational wave spectrum in heuristic and intuitive manners to illustrate the underlying physics. In Sec. IV, we give an improved calculation of the primordial gravitational wave spectrum in the SM, employing de Sitter inflation. Our final results are summarized in Figs. 4 and 5. In Appendix A we give useful formulas for the Bessel-type functions. In Appendix B we give analytical solutions of gravitational waves in some limiting cases. We define energy density of gravitational waves in Appendix C. The effect of neutrino free-streaming on the spectrum is formulated and explained in Appendix D. The numerical solution to the integro-differential equation is also presented. In Appendix E we give more detailed analytical accounts of numerical solutions of gravitational waves when the effective number of relativistic species changes. Units are chosen as $c = \hbar = k_B = 1$ and $\sqrt{8\pi G}$ is retained. Indices λ, μ, ν, ... run from 0 to 3, and i, j, k, ... run from 1 to 3. Over-dots are used for derivatives with respect to time throughout the paper. Primes are mainly used for derivatives with respect to conformal time, but sometimes with respect to arguments we are focusing on. Barred quantities are unperturbed parts of variables.

II. WAVE EQUATION, POWER SPECTRUM, AND ENERGY DENSITY

In this section we define the power spectrum, $\Delta_h^2(k)$, and relative spectral energy density, $\Omega_h(k)$, of the gravitational wave background. We do this because some authors use different conventions in the literature. For tensor perturbations on an isotropic, uniform and flat background spacetime, the metric is given by

$$ds^2 = a^2(\tau)[-d\tau^2 + (\delta_{ij} + h_{ij})dx^i dx^j], \tag{1}$$

$$g_{\mu\nu} = a^2(\tau)(\eta_{\mu\nu} + h_{\mu\nu}), \tag{2}$$

where

$$\eta_{\mu\nu} = \text{diag}(-1, 1, 1, 1), \qquad h_{00} = h_{0i} = 0, \qquad |h_{ij}| \ll 1. \tag{3}$$

Here and after we shall work in the transverse traceless (TT) gauge, which leaves only the tensor modes in perturbations, i.e. $h_{ij,j} = 0$ and $h^i{}_i = 0$. In the linear perturbation theory the TT metric fluctuations are gauge-invariant.[1] We shall denote the two independent polarization states of the perturbation as $\lambda = +, \times$ and sometimes suppress them when causing no confusion. We decompose h_{ij} into plane waves with the comoving wave number, $|\mathbf{k}| \equiv k$, as

$$h_{ij}(\tau, \mathbf{x}) = \sum_\lambda \int \frac{d^3 k}{(2\pi)^3} h_\lambda(\tau; \mathbf{k}) e^{i\mathbf{k}\cdot\mathbf{x}} \epsilon_{ij}^\lambda, \tag{4}$$

where ϵ_{ij}^λ is the polarization tensor and $\lambda = +, \times$. The equation for the wave amplitude, $h_\lambda(\tau; \mathbf{k}) \equiv h_{\lambda,\mathbf{k}}$, is obtained by requiring the perturbed metric [Eq. (2)] to satisfy the Einstein equation to $\mathcal{O}(h)$. One finds that $\delta G_{ij} = 8\pi G \delta T_{ij}$ in the linear order [29] yields

$$-\frac{1}{2} h_{ij;\nu}{}^{;\nu} = 8\pi G \Pi_{ij}, \tag{5}$$

where $\Pi_{ij}(t, \mathbf{x})$ is the anisotropic part of the stress tensor, defined by writing the spatial part of the perturbed energy-momentum tensor as

$$T_{ij} = p g_{ij} + a^2 \Pi_{ij}, \tag{6}$$

where p is pressure. For a perfect fluid $\Pi_{ij} = 0$, but this would not be true in general. In the cosmological context, the amplitude of gravitational waves is affected by anisotropic stress when neutrinos are freely streaming (less than $\sim 10^{10}$ K) [16–18,30–34]. As we only deal with tensor perturbations, h_{ij}, we may treat each component as a scalar quantity under general coordinate transformation, which means e.g. $h_{ij;\mu} = h_{ij,\mu}$. The left-hand side of Eq. (5) becomes

---

[1]In classic Refs. [27,28], $h_{ij} = 2H_{Tij}$ and $\Pi_{ij} = \bar{p}\pi_{Tij}$ for tensor perturbations, which are automatically gauge-invariant.

$$h_{ij;}{}^{\nu} = \bar{g}^{\mu\nu}(h_{ij,\mu\nu} - \Gamma^{\alpha}_{\mu\nu}h_{ij,\alpha}),$$

$$= -\ddot{h}_{ij} + \left(\frac{\nabla^2}{a^2}\right)h_{ij} - \left(\frac{3\dot{a}}{a}\right)\dot{h}_{ij}, \qquad (7)$$

where $\Gamma^0_{0\nu} = \Gamma^0_{\mu 0} = 0$, $\Gamma^0_{ij} = \delta_{ij}\dot{a}a$ and $\bar{g}^{ij} = a^{-2}\delta_{ij}$ have been used. Commas denote partial derivatives, while semicolons denote covariant derivatives in Eqs. (5) and (7). Transforming this equation into Fourier space, one obtains

$$\ddot{h}_{\lambda,\mathbf{k}} + \left(\frac{3\dot{a}}{a}\right)\dot{h}_{\lambda,\mathbf{k}} + \left(\frac{k^2}{a^2}\right)h_{\lambda,\mathbf{k}} = 16\pi G\Pi_{\lambda,\mathbf{k}}, \qquad (8)$$

where the Laplacian ∇^2 in the second term of (5) has been replaced by $-k^2$ in the third term of (8). The second term represents the effect of the expansion of the universe. Using conformal time derivatives ($' \equiv \frac{\partial}{\partial\tau}$), we may obtain

$$h''_{\lambda,\mathbf{k}} + \left(\frac{2a'}{a}\right)h'_{\lambda,\mathbf{k}} + k^2 h_{\lambda,\mathbf{k}} = 16\pi Ga^2\Pi_{\lambda,\mathbf{k}}. \qquad (9)$$

This is just the massless Klein-Gordon equation for a plane wave in an expanding space with a source term. Thus, each polarization state of the wave behaves as a massless, minimally coupled, real scalar field, with a normalization factor of $\sqrt{16\pi G}$ relating the two.

Next, let us consider the time evolution of the spectrum. After the fluctuations left the horizon, $k \ll aH$, Eq. (9) would become

$$\frac{h''_{\lambda,\mathbf{k}}}{h'_{\lambda,\mathbf{k}}} \approx -\frac{2a'}{a}, \qquad (10)$$

whose solution is

$$h_{\lambda,\mathbf{k}}(\tau) = A + B\int^{\tau}\frac{d\tau'}{a^2(\tau')}, \qquad (11)$$

where A and B are integration constants. Ignoring the second term that is a decaying mode, one finds that $h_{\lambda,\mathbf{k}}$ remains constant outside the horizon. Note that we have ignored the effect of anisotropic stress outside the horizon, as this term is usually given by causal mechanism which must vanish outside the horizon. Therefore, one may write a general solution of $h_{\lambda,\mathbf{k}}$ at any time as

$$h_{\lambda,\mathbf{k}}(\tau) \equiv h^{\mathrm{prim}}_{\lambda,\mathbf{k}}\mathcal{T}(\tau, k), \qquad (12)$$

where $h^{\mathrm{prim}}_{\lambda,\mathbf{k}}$ is the primordial gravitational wave mode that left the horizon during inflation. The transfer function, $\mathcal{T}(\tau, k)$, then describes the subhorizon evolution of gravitational wave modes after the modes entered the horizon. The transfer function is normalized such that $\mathcal{T}(\tau, k) \to 1$ as $k \to 0$. The power spectrum of gravitational waves, $\Delta^2_h(k)$, may be defined as

$$\langle h_{ij}(\tau, \mathbf{x})h^{ij}(\tau, \mathbf{x})\rangle = \int\frac{dk}{k}\Delta^2_h(\tau, k), \qquad (13)$$

which implies

$$\Delta^2_h(\tau, k) = \frac{2k^3}{2\pi^2}\sum_{\lambda}\langle|h_{\lambda,\mathbf{k}}(\tau)|^2\rangle. \qquad (14)$$

Using Eq. (12), one may write the time evolution of the power spectrum as

$$\Delta^2_h(\tau, k) \equiv \Delta^2_{h,\mathrm{prim}}[\mathcal{T}(\tau, k)]^2, \qquad (15)$$

where

$$\Delta^2_{h,\mathrm{prim}} = \frac{2k^3}{2\pi^2}\sum_{\lambda}\langle|h^{\mathrm{prim}}_{\lambda,\mathbf{k}}|^2\rangle = \frac{16}{\pi}\left(\frac{H_{\mathrm{inf}}}{m_{Pl}}\right)^2. \qquad (16)$$

We have used the prediction for the amplitude of gravitational waves from de Sitter inflation at the last equality, and H_{inf} is the Hubble constant during inflation. One may easily extend this result to slow-roll inflation models.

The energy density of gravitational waves is given by the 0-0 component of stress-energy tensor of gravitational waves:

$$\rho_h(\tau) = \frac{\langle h'_{ij}(\tau, \mathbf{x})h^{ij\prime}(\tau, \mathbf{x})\rangle}{32\pi Ga^2(\tau)}. \qquad (17)$$

The relative spectral energy density, $\Omega_h(\tau, k)$, is then given by the Fourier transform of energy density, $\tilde{\rho}_h(\tau) \equiv \frac{d\rho_h}{d\ln k}$, divided by the critical density of the universe, $\rho_{\mathrm{cr}}(\tau)$ (see Appendix C for full derivation):

$$\Omega_h(\tau, k) \equiv \frac{\tilde{\rho}_h(\tau, k)}{\rho_{\mathrm{cr}}(\tau)} = \frac{\Delta^2_{h,\mathrm{prim}}}{12a^2(\tau)H^2(\tau)}[\mathcal{T}'(\tau, k)]^2. \qquad (18)$$

Note that $\Omega_h(k)$ is often defined as $\Omega_h(\tau, k) = [(\Delta^2_{h,\mathrm{prim}})/(12a^2(\tau)H^2(\tau))]k^2[\mathcal{T}(\tau, k)]^2 = [k^2/(12a^2(\tau)H^2(\tau))]\Delta^2_h(\tau, k)$ in the literature [10,22,35]. This definition is not compatible with the 0-0 component of stress-energy tensor; however, it is a good approximation when the modes are deep inside the horizon, $k \gg aH$. Let us briefly explain a relation between these two definitions. The transfer function is usually given by Bessel-type functions, $\mathcal{T}(x) = \frac{1}{x^n}[Aj_n(x) + By_n(x)]$. The conformal time derivative of the transfer function is thus given by $\frac{d}{d\tau}\mathcal{T}(x) = -\frac{k}{x^n}[Aj_{n+1}(x) + By_{n+1}(x)]$, where $x \equiv k\tau$. Therefore, in the limit that the modes are deep inside the horizon, $k \gg aH$, one obtains $\Omega_h(k) = [(\Delta^2_{h,\mathrm{prim}})/(12a^2(\tau)H^2(\tau))][\mathcal{T}'(\tau, k)]^2 \approx [(\Delta^2_{h,\mathrm{prim}})/(12a^2(\tau)H^2(\tau))]k^2[\mathcal{T}(\tau, k)]^2$, which agrees with the definition of $\Omega_h(k)$ in [10,22,35]. The difference between Ω_h and $k^2\Delta^2_h$ would affect the prediction only at the largest scales, where both the overall amplitude and phases are different. (The phases are shifted by $\pi/2$.)

Figure 1 shows a numerical calculation of Eq. (18) for $\Omega_m = 1 - \Omega_r$, $\Omega_r h^2 = 4.15 \times 10^{-5}$, and $h = 0.7$. We ignored the contribution from dark energy, which is only important at the lowest frequency regime that we are not interested in in this paper. One may understand the basic features in this numerical result as follows. Energy density
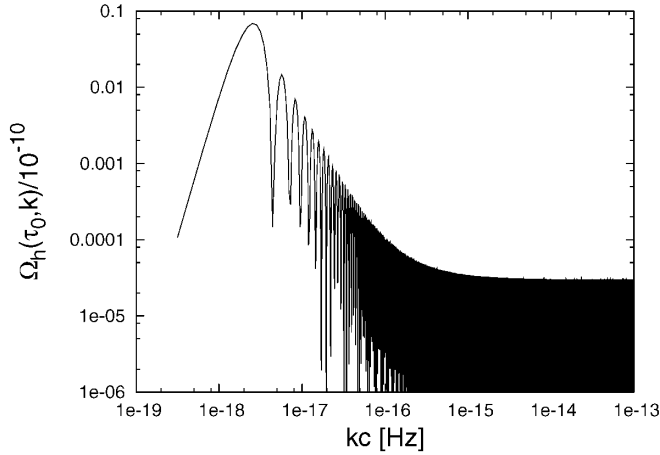
FIG. 1. The primordial gravitational wave spectrum at present, $\tau = \tau_0$, as a function of the comoving wavenumber, k (or kc in units of Hertz). The frequency of gravitational waves observed today is related to k by $f_0 = kc/2\pi$. The spectrum at large wavenumber is exactly scale-invariant as we have assumed de Sitter inflation. In this figure we have not taken into account the effects of the change in effective relativistic degrees of freedom or neutrino free-streaming.

of gravitational waves evolves just like that of radiation inside the horizon, $\tilde{\rho}_h(\tau, k) \propto a^{-4}$, for $k \gg aH$. This implies that the relative spectral energy density, $\Omega_h(\tau, k)$, inside the horizon remains independent of time during the radiation era while it decreases as $\Omega_h(\tau, k) \propto a^{-1}$ during the matter era. Therefore, the modes that entered the horizon during the matter era *later* would decay *less*. As the low frequency modes represent the modes that entered the horizon at late times, $\Omega_h(\tau, k)$ rises toward lower frequencies. On the other hand, $\Omega_h(\tau, k)$ at $k \gtrsim 10^{-15}$ Hz is independent of k. These are the modes that entered the horizon during the radiation era for which $\Omega_h(\tau, k)$ was independent of time. After the matter-radiation equality all of these modes suffered the same amount of redshift, and thus the shape of $\Omega_h(\tau, k)$ still remains scale-invariant at $k \gtrsim 10^{-15}$ Hz.

These qualitative arguments may be made more quantitative by using the following analytical solutions of $\Omega_h(\tau, k)$ for three different regimes (see Appendix B for derivation):

$$\Omega_h(\tau < \tau_{\rm eq}, k > k_{\rm eq}) = \frac{\Delta_{h,\rm prim}^2 a^2}{12 H_{\rm eq}^2 a_{\rm eq}^4} k^2 [j_1(k\tau)]^2, \quad (19)$$

$$\Omega_h(\tau > \tau_{\rm eq}, k > k_{\rm eq}) = \frac{\Delta_{h,\rm prim}^2 a}{12 H_0^2 a_0^3} k^2 \frac{\tau_{eq}^2}{\tau^2} [A(k) j_2(k\tau)$$
$$+ B(k) y_2(k\tau)]^2, \quad (20)$$

$$\Omega_h(\tau > \tau_{\rm eq}, k < k_{\rm eq}) = \frac{\Delta_{h,\rm prim}^2 a}{12 H_0^2 a_0^3} k^2 \left[\frac{3 j_2(k\tau)}{k\tau} \right]^2, \quad (21)$$

where $\tau_{\rm eq}$ is the conformal time at the matter-radiation equality, $k_{\rm eq}$ is the comoving wavenumber of the modes that entered the horizon at equality, and $j_0'(x) = -j_1(x)$ and $[\frac{j_1(x)}{x}]' = -\frac{j_2(x)}{x}$ have been used to compute $\mathcal{T}'(\tau, k)$. (Spherical Bessel functions are given in Appendix A.) The first solution [Eq. (19)] describes $\Omega_h(\tau, k)$ during radiation era for the modes that entered the horizon before $\tau_{\rm eq}$. This solution is of course not relevant to what we observe today. (We do not live in the radiation era.) The second [Eq. (20)] and third [Eq. (21)] solutions describe $\Omega_h(\tau, k)$ during matter era for the modes that entered the horizon before and after $\tau_{\rm eq}$, respectively. The k-dependent coefficients $A(k)$ and $B(k)$ are given in Eq. (B9) and (B10), respectively. While the expression is slightly complicated, one can find that the second solution is independent of k when the oscillatory part is averaged out, which explains a scale-invariant spectrum at high frequencies, $k > k_{\rm eq} \sim 10^{-15}$ Hz. On the other hand, the third solution gives $\Omega_h(\tau, k) \propto k^{-2}$, which explains the low frequency spectrum.

Figure 1 (and its extension to slow-roll inflation which yields a small tilt in the overall shape of the spectrum) has been widely referred to as the prediction from the standard model of cosmology. However, as we shall show in the subsequent sections, the standard model of cosmology actually yields much richer gravitational wave spectrum with more characteristic features in it.

III. THE EFFECTIVE RELATIVISTIC DEGREES OF FREEDOM: g_*

It is often taken for granted that energy density of the universe evolves as $\rho \propto a^{-4}$ during the radiation era. This is exactly what caused a scale-invariant spectrum of $\Omega_h(k)$ at $k > k_{\rm eq}$. However, $\rho \propto a^{-4}$ does not always hold even during the radiation era, as some particles would become nonrelativistic before the others and stop contributing to the radiation energy density.

During the radiation era many kinds of particles interacted with photons frequently so that they were in thermal equilibrium. In an adiabatic system, the entropy per unit comoving volume must be conserved [36];

$$S(T) = s(T) a^3(T) = \text{constant}, \quad (22)$$

where

$$s(T) = \frac{2\pi^2}{45} g_{*s}(T) T^3.$$

The entropy density, $s(T)$, is given by the energy density and pressure; $s = (\rho + p)/T$. The energy density and pressure in such a plasma-dominant universe are given by

$$\rho(T) = \frac{\pi^2}{30} g_*(T) T^4, \quad (23)$$

$$p(T) = \frac{1}{3}\rho(T), \tag{24}$$

respectively, where we have defined the "effective number of relativistic degrees of freedom", g_* and g_{*s}, following [36]. These quantities, g_* and g_{*s}, count the (effective) number of relativistic species contributing to the radiation energy density and entropy, respectively. One may call either (or both) of the two the effective number of relativistic degrees of freedom. Eqs. (22) and (23) immediately imply that energy density of the universe during the radiation era should evolve as

$$\rho \propto g_* g_{*s}^{-4/3} a^{-4}. \tag{25}$$

Therefore, unless g_* and g_{*s} are independent of time, the evolution of ρ would deviate from $\rho \propto a^{-4}$. In other words, the evolution of ρ during the radiation era is sensitive to how many relativistic species the universe had at a given epoch. As the wave equation of gravitational waves contains $(a'/a)h'_{\lambda,k}$, the solution of $h_{\lambda,k}$ would be affected by g_* and g_{*s} via the Friedman equation:

$$\frac{a'(\tau)}{a^2} = H_0 \sqrt{\left(\frac{g_*}{g_{*0}}\right)\left(\frac{g_{*s}}{g_{*s0}}\right)^{-4/3} \Omega_r \left(\frac{a}{a_0}\right)^{-4} + \Omega_m \left(\frac{a}{a_0}\right)^{-3}}. \tag{26}$$

Although the interaction rate among particles and antiparticles is assumed to be fast enough (compared with the expansion rate) to keep them in thermal equilibrium, the interaction is assumed to be weak enough for them to be treated as ideal gases. In the case of an ideal gas at temperature T, each particle species of a given mass, $m_i = x_i T$, would contribute to g_* and g_{*s} the amount given by

$$g_{*,i}(T) = g_i \frac{15}{\pi^4} \int_{x_i}^{\infty} \frac{(u^2 - x_i^2)^{1/2}}{e^u \pm 1} u^2 du, \tag{27}$$

$$g_{*s,i}(T) = g_i \frac{15}{\pi^4} \int_{x_i}^{\infty} \frac{(u^2 - x_i^2)^{1/2}}{e^u \pm 1}\left(u^2 - \frac{x_i^2}{4}\right) du, \tag{28}$$

where the sign is $+$ for bosons and $-$ for fermions.

Here, g_i is the number of helicity states of the particle and antiparticle. Note that an integral variable is defined as $u \equiv E/T$, where $E = \sqrt{|\mathbf{p}|^2 + m^2}$. We assume that the chemical potential, μ_i, is negligible. One might also define a similar quantity for the number density,

$$n(T) = \frac{\zeta(3)}{\pi^2} g_{*n} T^3, \tag{29}$$

where $\zeta(3) \simeq 1.20206$ is the Riemann zeta function of 3. Each species would contribute to g_{*n} by

$$g_{*n,i}(T) = g_i \frac{1}{2\zeta(3)} \int_{x_i}^{\infty} \frac{(u^2 - x_i^2)^{1/2}}{e^u \pm 1} u \, du. \tag{30}$$

The effective number of relativistic degrees of freedom is then given by the temperature-weighted sum of all particle contributions:

$$g_*(T) = \sum_i g_{*,i}(T)\left(\frac{T_i}{T}\right)^4, \qquad g_{*s}(T) = \sum_i g_{*s,i}(T)\left(\frac{T_i}{T}\right)^3,$$

$$g_{*n}(T) = \sum_i g_{*n,i}(T)\left(\frac{T_i}{T}\right)^3, \tag{31}$$

where we have taken into account the possibility that each species i may have a thermal distribution with a different temperature from that of photons. The most famous example is neutrinos: $T_\nu = (\frac{4}{11})^{1/3} T_\gamma$. Neutrinos are cooler than photons at temperatures below MeV scale due to photon heating from electron-positron annihilation.

Figure 2 shows the evolution of g_* as a function of temperature. We have included all the particles in the SM of elementary particles, as listed in Table I. (Note that we assume that the mass of Higgs bosons is 114 GeV, which is the current lower bound from experiments.) We neglected hadrons whose mass is heavier than pions. In addition to the particles in the SM, one may also include particles in supersymmetric models. Superpartners in the minimal extension of supersymmetric standard model (MSSM) would carry almost the same g_* as that carried by particles within the SM. Figure 3 shows the evolution of a'. If g_* and g_{*s} were constant, a' would also be constant during the radiation era; however, the evolution of a' reveals a series of jumps due to the change in g_* and g_{*s}.

Interactions between particles would change the ideal gas result obtained above, and one cannot use Eqs. (27), (28), and (31) to calculate g_* or g_{*s}. Instead, one needs to extract g_* and g_{*s} directly from energy density and entropy which would be calculated using detailed numerical simu-
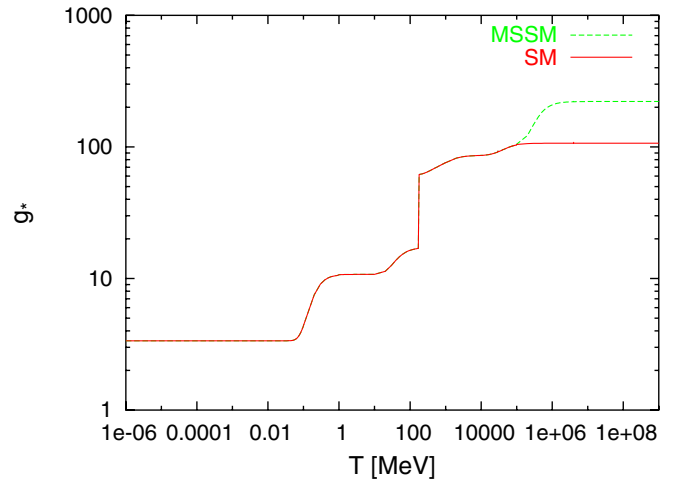
FIG. 2 (color online). Evolution of the effective number of relativistic degrees of freedom contributing to energy density, g_*, as a function of temperature. The solid and dashed lines represent g_* in the SM and in the minimal extension of SM, respectively. At the energy scales above ~ 1 TeV, $g_*^{\mathrm{SM}} = 106.75$ and $g_*^{\mathrm{MSSM}} \simeq 220$. At the energy scales below ~ 0.1 MeV, $g_* = 3.3626$ and $g_{*s} = 3.9091$; $g_* = g_{*s}$ otherwise.

TABLE I. Particles in the SM and their mass and helicity states.

Particle	Rest mass [MeV]	The number of helicity states: g_i
γ	0	2
$\nu, \bar{\nu}$	0	6
e^+, e^-	0.51	4
μ^+, μ^-	106	4
π^+, π^-	135	2
π^0	140	1
gluons	0	16
$u, \bar{u}$	5	12
$d, \bar{d}$	9	12
$s, \bar{s}$	115	12
$c, \bar{c}$	1.3×10^3	12
τ^+, τ^-	1.8×10^3	4
$b, \bar{b}$	4.4×10^3	12
W^+, W^-	80×10^3	6
Z	91×10^3	3
H	114×10^3	1
$t, \bar{t}$	174×10^3	12
SUSY particles	$\sim 1 \times 10^6$	~ 110

lations of particle interactions. For example, above the critical temperature of quark gluon plasma (QGP) phase transition, most of g_* is carried by color degrees of freedom. The dominant correction therefore comes from the colored sector of the SM, whereas corrections from the weak charged sector are suppressed by the masses of weak gauge bosons. Since physics of QCD correction is still uncertain and beyond the scope of this paper, we shall ignore this effect and treat it as an ideal gas case. The effects of particle interactions on g_* have been investigated by [15,37,38].
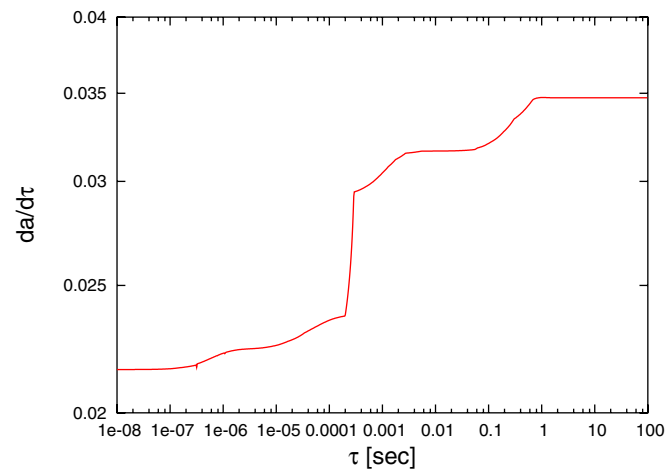

FIG. 3 (color online). Evolution of a' as a function of the conformal time. If g_* and g_{*s} were constant, $\rho \propto a^{-4}$ and a' would also be constant.

A. Heuristic argument based on background density

Before presenting the full numerical results, let us briefly describe how g_* and g_{*s} would affect the shape of $\Omega_h(\tau_0, k)$. In Sec. II, we discussed how the expansion of the universe would affect $\Omega_h(\tau_0, k)$. While energy density of the universe during the radiation era is affected by g_* and g_{*s} as $\rho_{cr} \propto g_* g_{*s}^{-4/3} a^{-4}$, energy density of gravitational waves always evolves as $\tilde{\rho}_h(\tau, k) \propto a^{-4}$ inside the horizon, $k \gg aH$, regardless of g_* or g_{*s}. (Gravitons are not in thermal equilibrium with other particles.) This difference in the evolution of $\tilde{\rho}_h$ and ρ_{cr} significantly modifies a scale-invariant spectrum of $\Omega_h(\tau_0, k)$ at $k > k_{eq}$.

Let us consider a gravitational wave mode with k which entered the horizon at a given time, $\tau_{hc} < \tau_{eq}$ and temperature, $T = T_{hc}$, during the radiation era. After the mode entered the horizon the amplitude of this mode would be suppressed by the cosmological redshift. The relative spectral density at present would then be given by

$$\Omega_h(\tau_0, k > k_{eq}) = \Omega_h(\tau_{hc}, k)\Omega_{r0}\left[\frac{g_{*s}(T_{hc})}{g_{*s0}}\right]^{-4/3}$$
$$\times \left[\frac{g_*(T_{hc})}{g_{*0}}\right], \tag{32}$$

where Ω_r denotes the relative energy density of radiation and the subscript "0" denotes the present-day value. This equation helps us understand how g_* and g_{*s} would affect $\Omega_h(\tau_0, k)$. For a given wavenumber, k, there would be one horizon-crossing epoch, τ_{hc}. The amount by which the relative spectral energy density of that mode would be suppressed depends on g_* and g_{*s} at τ_{hc}. The mode that entered the horizon earlier should experience larger suppression, as g_* and g_{*s} would be larger than those for the mode that entered the horizon later. (The effective number of relativistic degrees of freedom is larger at earlier times—see Fig. 2.) As g_* and g_{*s} are equal for $T \gtrsim 0.1$ MeV and nearly the same otherwise ($g_* = 3.3626$ and $g_{*s} = 3.9091$ for $T \lesssim 0.1$ MeV), we expect that suppression factor is given by $(g_*/g_{*0})^{-1/3}$ to a good approximation. The modes that entered the horizon during the matter era should not be affected by g_* or g_{*s}, as they do not change during the matter era.

B. More rigorous argument using analytical solutions

In this subsection we derive Eq. (32) using a more rigorous approach. Let us go back to the wave equation [Eq. (9)], and rewrite it using a new field variable, $\mu_k \equiv a h_k$:

$$\mu_k'' + \left(k^2 - \frac{a''}{a}\right)\mu_k = 16\pi G a^3 \Pi_k. \tag{33}$$

Note that we have suppressed the subscript for polarization, λ. To find a solution for μ_k, we must solve the Friedman equation as well:

$$\left(\frac{a'}{a^2}\right)^2 = \frac{8\pi G}{3}\rho_r = H_0^2 \frac{g_*}{g_{*0}}\left(\frac{g_{*s}}{g_{*s0}}\right)^{-4/3}\left(\frac{a}{a_0}\right)^{-4}$$

$$\frac{a'}{a^2} = H_0\left(\frac{g_*}{g_{*0}}\right)^{1/2}\left(\frac{g_{*s}}{g_{*s0}}\right)^{-2/3}\left(\frac{a}{a_0}\right)^{-2}$$

$$\frac{a - a_0}{a_0} = a_0 H_0 \int_{\tau_0}^{\tau} d\tau'\left(\frac{g_*}{g_{*0}}\right)^{1/2}\left(\frac{g_*}{g_{*0}}\right)^{-2/3}, \tag{34}$$

where the subscript 0 denotes some reference epoch during the radiation era. (While 0 means the present epoch in the other sections, we use it to mean some epoch during the radiation era in this section only.) To proceed further, we need to specify the evolution of g_* and g_{*s}. While we have numerical data for the evolution of these quantities, we make an approximation here to make the problem analytically solvable. Since $g_*(\tau)$ decreases monotonically as the universe expands, one may try a reasonable *ansatz*, $g_* \propto \tau^{-6n}$, to obtain analytical solutions. We shall also assume $g_* = g_{*s}$ and $\Pi_k = 0$ for simplicity in this section. (At temperatures below 2 MeV, free-streaming of neutrinos generates anisotropic stress, $\Pi_k \neq 0$. Also, the temperature of neutrinos is different from that of photons below electron-positron annihilation temperature, and thus $g_* \neq g_{*s}$ below ~0.51 MeV.) This model gives

$$\frac{a''}{a} \simeq \frac{g_*^{-7/6}\,|\,g_*'\,|}{6\int_{\tau_0}^{\tau} d\tau' g_*^{-1/6}} \simeq \frac{n}{\tau^2}(1 + n), \tag{35}$$

where the primes denote derivatives with respect to τ, and the term $\frac{n}{\tau_0^2}(1 + n)$ has been neglected in the last line, assuming $\tau \ll \tau_0$. This form of a''/a allows us to find an analytical solution to Eq. (33):

$$h_k(\tau) = \frac{\mu_k(\tau)}{a} = A(k)\frac{j_n(k\tau)}{(k\tau)^n} + B(k)\frac{y_n(k\tau)}{(k\tau)^n}, \tag{36}$$

where $A(k)$ and $B(k)$ are the normalization constants that should be determined by the appropriate boundary conditions. Note that $n = 0$ and $n = 1$ correspond to the solutions for the radiation era and the matter era, respectively.

Let us consider a model of the radiation-dominated universe in which there was a brief period of time during which g_* suddenly decreased as a power-law in time, $g_* \propto \tau^{-6n}$. Outside of this period g_* is a constant. Suppose that g_* changed between $\tau = \tau_2$ and $\tau_1 > \tau_2$. (The change in g_* began at $\tau = \tau_2$ and completed at τ_1.) The modes that entered the horizon after τ_1 do not know anything about the change in g_*. The solution for such modes is therefore given by the usual solution during the radiation era,

$$h_k^{\mathrm{out}}(\tau) = h_k^{\mathrm{prim}} j_0(k\tau). \tag{37}$$

How about the modes that entered the horizon before τ_2? The solution for such modes is given by

$$h_k^{\mathrm{in}}(\tau) = h_k^{\mathrm{prim}} j_0(k\tau) \qquad (\tau < \tau_2), \tag{38}$$

$$h_k^{\mathrm{in}}(\tau) = \frac{h_k^{\mathrm{prim}}}{(k\tau)^n}[A(k)j_n(k\tau) + B(k)y_n(k\tau)] \tag{39}$$

$$(\tau_2 < \tau < \tau_1),$$

$$h_k^{\mathrm{in}}(\tau) = h_k^{\mathrm{prim}}\left(\frac{\tau_2}{\tau_1}\right)^n[C(k)j_0(k\tau) + D(k)y_0(k\tau)] \tag{40}$$

$$(\tau_1 < \tau).$$

It is convenient to define $\tau_* \equiv (\tau_1 + \tau_2)/2$ and $\Delta\tau \equiv \tau_1 - \tau_2$ to characterize the time of transition and its duration, respectively. Here, the superscript "in" denotes the modes that have already been *inside* the horizon at τ_*, while "out" denotes the modes that are still *outside* the horizon at τ_*. The coefficients, $A(k)$, $B(k)$, $C(k)$, and $D(k)$, are given by Eqs. (E1)–(E4) in Appendix E. By taking a ratio of Eqs. (37) and (40), we can find the amount of suppression in $h_k^{\mathrm{in}}(\tau > \tau_1)$ relative to $h_k^{\mathrm{out}}(\tau > \tau_1)$:

$$\frac{h_k^{\mathrm{in}}(\tau > \tau_1)}{h_k^{\mathrm{out}}(\tau > \tau_1)} = \left(\frac{\tau_2}{\tau_1}\right)^n[C(k) + D(k)y_0(k\tau)/j_0(k\tau)]$$

$$\approx \left(\frac{\tau_2}{\tau_1}\right)^n[C(k) + D(k)], \tag{41}$$

where we have ignored the oscillatory part of $y_0(k\tau)/j_0(k\tau)$. While $C(k)$ and $D(k)$ have fairly cumbersome expressions, the sum of the two has a simple limit, $[C(k) + D(k)]^2 \to 1$, for $\Delta\tau \to 0$, regardless of the value of n (see Appendix E). The energy density in gravitational waves then reflects the effect from the change of g_* as

$$\frac{\Omega_h^{\mathrm{in}}(\tau > \tau_1, k)}{\Omega_h^{\mathrm{out}}(\tau > \tau_1, k)} \approx \left[\frac{h_k^{\mathrm{in}}(\tau > \tau_1)}{h_k^{\mathrm{out}}(\tau > \tau_1)}\right]^2 \approx 1 - 2n\frac{\Delta\tau}{\tau_1}, \tag{42}$$

where we have used the subhorizon limit for $\Omega_h(k)$ and $\Delta\tau \ll \tau_2 < \tau_* < \tau_1$. On the other hand, $g_* \propto \tau^{-6n}$ gives

$$\frac{g_*^{\mathrm{in}}}{g_*^{\mathrm{out}}} \equiv \frac{g_*(\tau_2)}{g_*(\tau_1)} = \left(\frac{\tau_* - \Delta\tau/2}{\tau_* + \Delta\tau/2}\right)^{-6n} \approx 1 + 6n\frac{\Delta\tau}{\tau_*}. \tag{43}$$

Hence, combining Eqs. (42) and (43), we finally obtain the desired result

$$\frac{\Omega_h^{\mathrm{in}}(k)}{\Omega_h^{\mathrm{out}}(k)} \approx \left(\frac{g_*^{\mathrm{in}}}{g_*^{\mathrm{out}}}\right)^{-1/3}, \tag{44}$$

for $\Delta\tau \ll \tau_*$. This result agrees with Eq. (32), which was obtained in the previous section (Sec. III A) using a more heuristic argument. (Note that we have assumed $g_* = g_{*s}$ in this section). In Eq. (32) there is an extra factor Ω_{r0}, which represents the time evolution of Ω_h from matter-radiation equality to the present epoch. We do not have this factor in Eq. (44), as both Ω_h^{in} and Ω_h^{out} are evaluated during the radiation era.

IV. PREDICTION FOR ENERGY DENSITY OF GRAVITATIONAL WAVES FROM THE STANDARD MODEL AND BEYOND

In Sec. III we have described how the evolution of the effective number of relativistic degrees of freedom would affect the shape of relative spectral energy density of primordial gravitational waves at present, $\Omega_h(\tau_0, k)$. In this section we present the full calculation of $\Omega_h(\tau_0, k)$, numerically integrating the wave equation together with the numerical data of g_* and g_{*s} (see Fig. 2).

Before we do this, there is another effect that one must take into account. While we have ignored anisotropic stress on the right-hand side of the wave Eq. (9) so far, free-streaming of relativistic neutrinos which have decoupled from thermal equilibrium at $T \lesssim 2$ MeV significantly contributes to anisotropic stress, damping the amplitude of primordial gravitational waves [18,32]. Calculations given in Appendix D show that neutrino anisotropic stress damps $\Omega_h(\tau_0, k)$ by 35.5% in the frequency region between $\simeq 10^{-16}$ and $\simeq 2 \times 10^{-10}$ Hz. The damping effect is much less significant below 10^{-16} Hz, as this frequency region probes the universe that is dominated by matter. One may understand this by looking at the right-hand side of Eq. (D23). Anisotropic stress is proportional to the fraction of the total energy density in neutrinos, $f_\nu(\tau)$, which is very small when the universe is matter dominated.

We show the results of full numerical integration in Figs. 4 and 5. The latter figure is just a zoom-up of interesting features in the former one. We find that $\Omega_h(\tau_0, k)$ oscillates very rapidly as $\sin^2(k\tau + \varphi)$, where φ is a phase constant. The cross term, $\sin k\tau \cos k\tau$, appeared as a beat in Fig. 1, while they are too small to see in Fig. 4. From observational point of view these oscillations will not be detectable, as observations are only sensitive to the average power over a few decades in frequency.

The damping effect due to neutrino free-streaming is evident below 2×10^{-10}, while one might also notice a minor wiggly feature at around 5×10^{-10} Hz. This feature is actually artificial. We implicitly assumed an instantaneous decoupling of neutrinos from the thermal plasma at $T_{\nu\,\text{dec}} = 2$ MeV, which resulted in the *surface* of decoupling that is extremely thin. This gave rise to dips and peaks corresponding to the waveform of gravitational waves at the decoupling time. (The envelope shape is somewhat similar to $-j_1(k)$ at around 5×10^{-10} Hz; more details are given in Appendix D.) Physically speaking, however, the last scattering surface of neutrinos is very thick, unlike for photons. (There is no "recombination" for neutrinos.) Therefore, the oscillatory feature would be smeared out when thickness of the decoupling surface is explicitly taken into account. To do this, one would need to solve the Boltzmann equation for neutrinos separately, including the effect of neutrino decoupling.

The effect of evolution of g_* and g_{*s} is also quite prominent. For example, big changes in g_* would occur
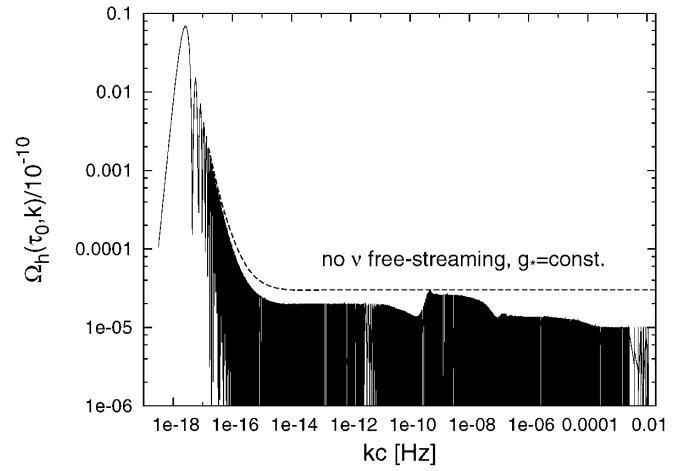

FIG. 4. The primordial gravitational wave spectrum at present, $\Omega_h(\tau_0, k)/10^{-10}$, as a function of the comoving wavenumber, k (or kc in units of Hertz). The frequency of gravitational waves observed today is related to k by $f_0 = kc/2\pi$. We have assumed a scale-invariant primordial spectrum and $\Omega_m = 1 - \Omega_r$, $\Omega_r = 4.15 \times 10^{-5} h^{-2}$, $h = 0.7$, and $E_{\text{inf}} = 10^{16}$ GeV. We have included the effects of the effective number of relativistic degrees of freedom and neutrino free-streaming. The dashed line shows the envelope of the previous calculations which ignored the change in the number of relativistic degrees of freedom and neutrino free-streaming (Fig. 1).

at the electron-positron annihilation epoch, ~ 0.51 MeV ($\sim 2 \times 10^{-11}$ Hz), as well as at the QGP to hadron gas phase transition epoch, ~ 180 MeV ($\sim 10^{-7}$ Hz) within the SM. The gravitational wave spectrum is suppressed by roughly 20% and 30% above the electron-positron annihilation and QGP phase transition scale, respectively. If supersymmetry existed above a certain energy scale, e.g., ~ 1 TeV ($\sim 1 \times 10^{-4}$ Hz), the spectrum would be suppressed by at least $\sim 20\%$ (for $N = 1$ supersymmetry)
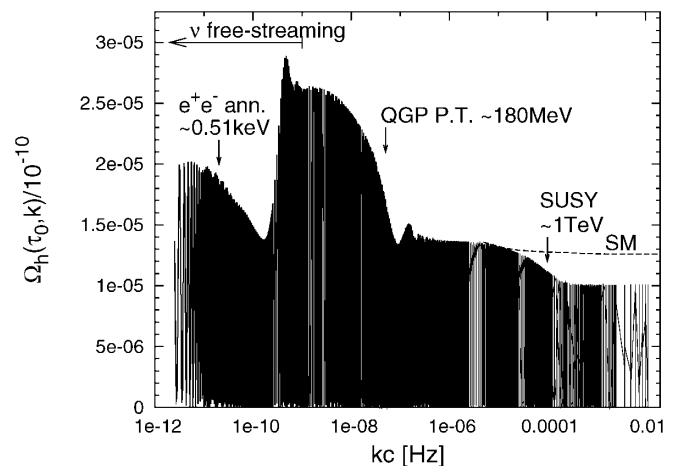

FIG. 5. A blow-up of Fig. 4. Note that density of vertical lines shows density of sampling points at which we evaluate $\Omega_h(\tau_0, k)$. The dashed line shows the envelope of the spectrum in the SM of elementary particles.

above that frequency. We also find additional features at the QGP phase transition scale, $\sim 10^{-7}$ Hz, similar to the features at $\sim 5 \times 10^{-10}$ Hz caused by our assumption about instantaneous decoupling of neutrinos. The feature at the QGP phase transition is nevertheless not artificial—as the QGP phase transition is expected to have happened in a short time period, the instantaneous transition would be a good approximation, unlike for neutrinos.

One may approximately relate the horizon-crossing temperature of the universe to the frequency of the gravitational waves [13,39]. The horizon-crossing mode, $k_{\mathrm{hc}} = a_{\mathrm{hc}} H_{\mathrm{hc}}$, is related to the temperature at that time by $H_{\mathrm{hc}}^2 = \frac{8\pi^3 G}{90} g_{*,\mathrm{hc}} T_{\mathrm{hc}}^4$. Then using entropy conservation, $g_{*s,\mathrm{hc}} a_{\mathrm{hc}}^3 T_{\mathrm{hc}}^3 = g_{*s0} a_0^3 T_0^3$, one obtains the following conversion factor from the temperature of the universe to the frequency of gravitational waves observed today:

$$f_0 = 1.65 \times 2\pi \times 10^{-7} \left(\frac{T_{\mathrm{hc}}}{1 \text{ GeV}}\right)\left[\frac{g_{*s}(T_{\mathrm{hc}})}{100}\right]^{-1/3}$$
$$\times \left[\frac{g_*(T_{\mathrm{hc}})}{100}\right]^{1/2} \text{ Hz}, \tag{45}$$

which was derived in [13,39]. (If we take $\epsilon \equiv \frac{1}{2\pi}$ in [39], their equation (156) agrees with the one above.) Throughout this paper we have been using the comoving wavenumber, k (or kc in units of Hertz), which is related to the conventional frequency by $2\pi f_0 = kc/a_0$, where a_0 is the present-day scale factor and c is the speed of light. We use k in this paper, rather than f_0, as k is what enters into the wave equation that we solve numerically.

V. DISCUSSION AND CONCLUSION

We have calculated the primordial gravitational wave spectrum, fully taking into account the evolution of the effective relativistic degrees of freedom and neutrino free-streaming, which were ignored in the previous calculations. The formalism and results given in this paper are based on solid physics and can be extended to primordial gravitational waves produced in any inflationary models and high energy particle physics models. As is seen in Figs. 4 and 5, the spectrum is no longer scale-invariant, but has complex features in it. Whatever physics during inflation is, one must include the evolution of the effective relativistic degrees of freedom and neutrino free-streaming.

[14] studied the gravitational wave spectrum at the QGP phase transition assuming the first order instantaneous model as well as the second order crossover model, and found 30% suppression of the energy density spectrum, which is consistent with our calculation. [40] studied the effect of entropy production from e.g., decay of massive particles in the early universe on the energy density spectrum. We have not included this effect in our calculations, as the late-time entropy production is not predicted within the SM. [41] studied the effect of changes in the equation of state of the universe on the energy density spectrum. While they included the effect of neutrino free-streaming, they did not include the evolution of g_*. Instead, they explored general possibilities that the equation of state might be modified by trace anomaly or interactions among particles. They also considered damping of gravitational waves due to anisotropic stress of some hypothetical particles. Our calculations are different from theirs, as we took into account explicitly all the particles in the SM and the minimal extension of the SM, but did not include any exotic physics beyond that.

Let us mention a few points that would merit further studies. At the energy scales where supersymmetry is unbroken (if it exists), say TeV scales and above, the number of relativistic degrees of freedom, g_*, should be at least doubled, and would cause suppression of the primordial gravitational waves (Fig. 5 for $N = 1$ supersymmetry). If, for instance, $N = 8$ is the number of internal supersymmetric charges, ~ 250 copies of SM particles would appear in this theory. This would suppress the spectrum by 85% at the high frequency region (above $\sim 10^{-4}$ Hz) compare to the SM, though the details depend on models. Since we still do not have much idea about a *true* supersymmetric model and its particle rest mass, the search for the primordial gravitational waves would help to constrain the effective number of relativistic degrees of freedom $g_*(T)$ above the TeV scales.

In an extremely high frequency region, k_{rh}, the gravitational wave spectrum should provide us with unique information about the reheating of the universe after inflation. If the inflaton potential during reheating is monomial, $V(\phi) \propto \phi^n$, the equation of state during reheating is given by $p_\phi = \alpha(n)\rho_\phi$, where $\alpha(n) = \frac{n-2}{n+2}$. Since the equation of state determines the expansion law of that epoch, one obtains the frequency dependence of the gravitational wave spectrum as $\Omega_h \propto k^{(n-4)/(n-1)}$. In an extremely low frequency region (below $\sim 10^{-18}$ Hz), on the other hand, dark energy dominates the universe and affects the spectrum [42]. Acceleration of the universe reduces the amplitude of gravitational waves that enter the horizon at this epoch; however, we will not be able to observe modes as big as the size of the horizon today.

The signatures of the primordial gravitational waves may be detected only by the CMB polarization in the low frequency region, $\lesssim 10^{-16}$ Hz. For the higher frequency region, however, direct detection of the gravitational waves would be necessary, and it should allow us to search for a particular cosmological event by arranging an appropriate instrument, as the events during the radiation era are imprinted on the spectrum of the primordial gravitational waves.

APPENDIX A: SPHERICAL BESSEL-TYPE FUNCTIONS

We present some formulas for Bessel-type functions used in this paper.

$$\frac{d}{dx}\left[\frac{z_n(x)}{x^n}\right] = -\frac{z_{n+1}(x)}{x^n}, \quad \frac{d}{dx}[x^{n+1}z_n(x)] = x^{n+1}z_{n-1}(x),$$

$$(A1)$$

where $z_n(x)$ can be spherical Bessel functions, spherical Neumann functions, Bessel functions, and Neumann functions.

Spherical Bessel functions and spherical Neumann functions are related by

$$y_n(x) = (-1)^{n+1}j_{-n-1}(x).$$

$$(A2)$$

Their asymptotic forms are

$$j_n(x) \approx \frac{\sin(x - n\pi/2)}{x}, \qquad y_n(x) \approx -\frac{\cos(x - n\pi/2)}{x}$$

$$(A3)$$

for $x \gg 1$. If n is even, $j_n(x) \approx \pm j_0(x)$ and $y_n(x) \approx \pm y_0(x)$. If n is odd, $j_n(x) \approx \pm y_0(x)$ and $y_n(x) \approx \pm j_0(x)$. The first and second kinds of spherical Hankel functions are defined as

$$h_n^{(1)}(x) = j_n(x) + iy_n(x), \qquad h_n^{(2)}(x) = j_n(x) - iy_n(x).$$

$$(A4)$$

Using elementary functions, we have

$$j_0(x) = \frac{\sin x}{x},$$

$$(A5)$$

$$j_1(x) = \frac{1}{x}\left[\frac{\sin x}{x} - \cos x\right],$$

$$(A6)$$

$$j_2(x) = \frac{1}{x}\left[\left(\frac{3}{x^2} - 1\right)\sin x - \frac{3}{x}\cos x\right],$$

$$(A7)$$

$$y_0(x) = -\frac{\cos x}{x},$$

$$(A8)$$

$$y_1(x) = -\frac{1}{x}\left[\frac{1}{x}\cos x + \sin x\right],$$

$$(A9)$$

$$y_2(x) = -\frac{1}{x}\left[\left(\frac{3}{x^2} - 1\right)\cos x + \frac{3}{x}\sin x\right],$$

$$(A10)$$

$$h_1^{(1)}(x) = -\frac{1}{x}\left(1 + \frac{i}{x}\right)e^{-ix},$$

$$(A11)$$

$$h_1^{(2)}(x) = -\frac{1}{x}\left(1 - \frac{i}{x}\right)e^{-ix}.$$

$$(A12)$$

APPENDIX B: ANALYTICAL SOLUTIONS OF WAVE EQUATION

In this Appendix we shall discuss solutions of the equation of motion [Eq. (9)]. While we assume $\Pi_{ij} = 0$ in this Appendix, we shall treat $\Pi_{ij} \neq 0$ in Appendix D. Imposing appropriate boundary conditions [43], one obtains simple analytical solutions for tensor modes of fluctuations in the inflationary (de Sitter), radiation dominated (RD) and matter dominated (MD) universe, as

$$h_{\mathbf{k}}(\tau) = \frac{\sqrt{16\pi G}}{\sqrt{2ka}}\left(1 - \frac{i}{k\tau}\right)e^{-ik\tau}\alpha(\mathbf{k}),$$

$$= -\frac{\tau}{a}\sqrt{8\pi Gk}h_1^{(2)}(k\tau)\alpha(\mathbf{k}) \qquad \text{inflation,} \quad (B1)$$

$$h_{\mathbf{k}}(\tau) = [j_0(k\tau)]h_{\mathbf{k}}^{\text{prim}} \qquad \text{RD,} \qquad (B2)$$

$$h_{\mathbf{k}}(\tau) = \left[\frac{3j_1(k\tau)}{k\tau}\right]h_{\mathbf{k}}^{\text{prim}} \qquad \text{MD,} \qquad (B3)$$

where $\alpha(\mathbf{k})$ is a stochastic variable satisfying $\langle \alpha(\mathbf{k})\alpha^*(\mathbf{k}')\rangle = \delta^3(\mathbf{k} - \mathbf{k}')$, and spherical Bessel-type functions are given in Appendix A. We classify wave modes by their horizon crossing time, τ_{hc};

$$|\mathbf{k}| = k\begin{cases} > k_{\text{eq}} & \text{the modes that entered the horizon during RD: } \tau_{\text{hc}} < \tau_{\text{eq}} \\ < k_{\text{eq}} & \text{the modes that entered the horizon during MD: } \tau_{\text{hc}} > \tau_{\text{eq}} \end{cases},$$

$$(B4)$$

where τ_{eq} denotes the time at the matter-radiation equality, and τ_{hc} denotes the time when fluctuation modes crossed the horizon, $k\tau_{\text{hc}} = 1$. Notice that $|h_k(\tau)|^2$ for each solution (B1)–(B3) does not depend on time ($\equiv |h_k^{\text{prim}}|^2$) at the super-horizon scale, $|k\tau| \ll 1$.

The tensor mode fluctuations from the inflationary universe left the horizon and *froze out*. Its dimensionless spectrum is given from Eq. (B1) as

$$\Delta_h^2(k) \equiv 4k^3 \frac{|h_k^{\mathrm{inf}}|^2}{2\pi^2} = 64\pi G \left(\frac{H_{\mathrm{inf}} k\tau}{2\pi}\right)^2 \left(1 + \frac{1}{k^2\tau^2}\right)$$

$$\simeq \frac{16}{\pi}\left(\frac{H_{\mathrm{inf}}}{m_{\mathrm{Pl}}}\right)^2 \equiv 4k^3 \frac{|h_k^{\mathrm{prim}}|^2}{2\pi^2} \qquad \text{(B5)}$$

$$(|k\tau| \ll 1),$$

where H_{inf} is the Hubble parameter during inflation and $\tau = -1/(aH_{\mathrm{inf}})$ is used in the second equality. Note that the conventional factor 4 is from $\int \frac{dk}{k} \Delta_h^2(k) \equiv \langle h_{ij} h^{ij} \rangle = 2[\langle |h_+|^2 \rangle + \langle |h_\times|^2 \rangle] = 4|h|^2$, where $|h_{+,k}| = |h_{\times,k}| \equiv |h|$ is assumed [44]. From the Friedman equation during inflation, one obtains $H_{\mathrm{inf}}^2 \approx \frac{8\pi}{3m_{\mathrm{Pl}}^2} V(\phi)$, which gives $\Delta_{h,\mathrm{prim}}^2 \approx 10V(\phi)/m_{\mathrm{Pl}}^4$; thus $\Delta_{h,\mathrm{prim}}^2$ is sensitive to the shape of inflaton potential [10,12]. The dimensionless spectrum (B5) is nearly independent k. This is the famous prediction of the inflationary scenario known as a nearly scale-invariant spectrum. As long as we consider de Sitter inflation, the spectrum is exactly scale-invariant, i.e. $\propto k^0$ as ϕ is at rest.

Using the transfer function [Eq. (12)], we obtain the time evolution of the amplitude of gravitational waves as

$$\mathcal{T}(\tau < \tau_{\mathrm{eq}}, k > k_{\mathrm{eq}}) = j_0(k\tau), \qquad \text{(B6)}$$

$$\mathcal{T}(\tau > \tau_{\mathrm{eq}}, k > k_{\mathrm{eq}}) = \frac{\tau_{\mathrm{eq}}}{\tau}[A(k)j_1(k\tau) + B(k)y_1(k\tau)], \qquad \text{(B7)}$$

$$\mathcal{T}(\tau, k < k_{\mathrm{eq}}) = \frac{3j_1(k\tau)}{k\tau}, \qquad \text{(B8)}$$

where

$$A(k) = \frac{3}{2k\tau_{\mathrm{eq}}} - \frac{\cos 2k\tau_{\mathrm{eq}}}{2k\tau_{\mathrm{eq}}} + \frac{\sin 2k\tau_{\mathrm{eq}}}{(k\tau_{\mathrm{eq}})^2}, \qquad \text{(B9)}$$

$$B(k) = -1 + \frac{1}{(k\tau_{\mathrm{eq}})^2} - \frac{\cos 2k\tau_{\mathrm{eq}}}{(k\tau_{\mathrm{eq}})^2} - \frac{\sin 2k\tau_{\mathrm{eq}}}{2k\tau_{\mathrm{eq}}}. \qquad \text{(B10)}$$

Their conformal time derivatives are given as

$$\mathcal{T}'(\tau < \tau_{\mathrm{eq}}, k > k_{\mathrm{eq}}) = -kj_1(k\tau), \qquad \text{(B11)}$$

$$\mathcal{T}'(\tau > \tau_{\mathrm{eq}}, k > k_{\mathrm{eq}}) = -\frac{k\tau_{\mathrm{eq}}}{\tau}[A(k)j_2(k\tau) + B(k)y_2(k\tau)], \qquad \text{(B12)}$$

$$\mathcal{T}'(\tau, k < k_{\mathrm{eq}}) = -\frac{3j_2(k\tau)}{\tau}. \qquad \text{(B13)}$$

Equations (B6) and (B7) are the evolution of modes which entered the horizon during the radiation era, while Eq. (B8) is the evolution of modes which entered the horizon during the matter era. Coefficients $A(k)$ and $B(k)$ are obtained by equating a solution (B6) with (B7) and their first derivatives [(B11) and (B12)] at the matter-radiation equality.
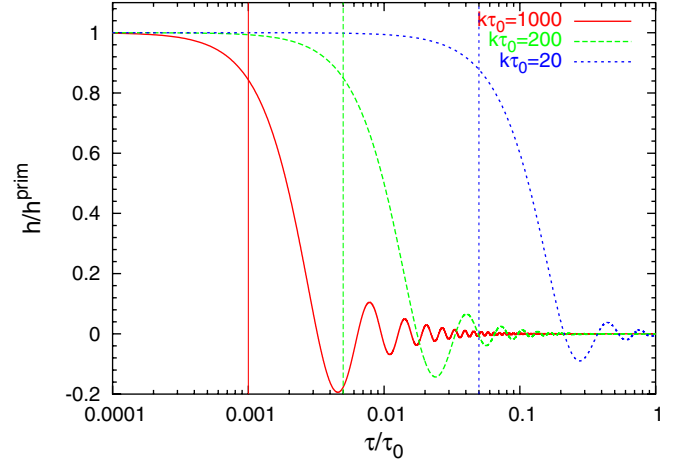

FIG. 6 (color online). Numerical solutions of tensor perturbations. The solid, dashed, and short-dashed lines show the high, medium, and low frequency modes, respectively. The higher k-modes enter the horizon earlier, and are damped more by the cosmological redshift. Vertical lines define the horizon-crossing time for each k-mode.

The transfer function for the intermediate regime, Eq. (B7), can be calculated numerically so that the two other limiting solutions match smoothly (See Fig. 1). If the wavelength of the gravitational waves is much shorter than the duration of the cosmological transition, a WKB approximation may be appropriate [32,45]. Here we just assumed the instantaneous transition to illustrate the main point. The analytical solutions as well as numerical solutions are presented and
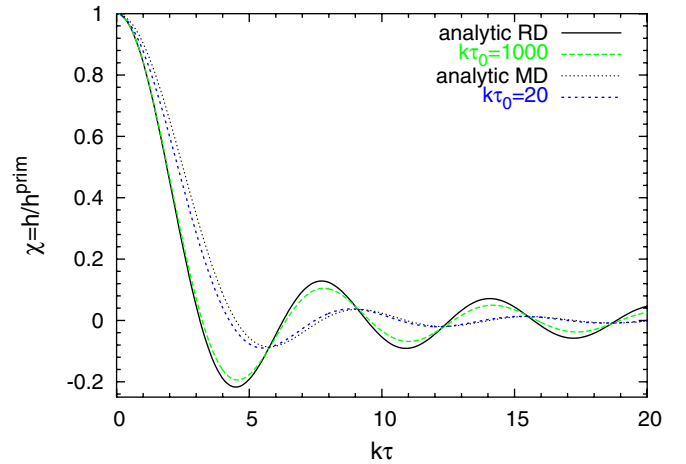

FIG. 7 (color online). Comparison between numerical solutions and analytical solutions of tensor perturbations. The dashed and short-dashed lines show numerical solutions of the high and low frequency modes, respectively. The higher k-modes enter the horizon earlier, and thus the numerical solution is well approximated by the analytical solution during the radiation era, $\chi(k\tau) = j_0(k\tau)$ (solid line). On the other hand, the lower k-modes enter the horizon much later, and thus the numerical solution is close to the analytical solution during the matter era, $\chi(k\tau) = 3j_1(k\tau)/k\tau$ (dotted line).

compared in Figs. 6 and 7. The higher k-modes enter the horizon earlier, and their amplitudes are damped more by the cosmological redshift.

APPENDIX C: THE RELATIVE SPECTRAL DENSITY: $\Omega_h(k)$

In this Appendix we shall define the energy-momentum tensor of gravitational waves following the argument and the definition in § 35.7 and § 35.13 of [46]. The Ricci tensor for the metric of the form given in Eq. (1) may be expanded in metric perturbations, h:

$$R_{\mu\nu} = \bar{R}_{\mu\nu} + R^{(1)}_{\mu\nu} + R^{(2)}_{\mu\nu} + \mathcal{O}(h^3), \qquad (C1)$$

where $R^{(1)}_{\mu\nu} \sim \mathcal{O}(h)$ and $R^{(2)}_{\mu\nu} \sim \mathcal{O}(h^2)$.

For the vacuum field equation, $R_{\mu\nu} = 0$. As the Einstein equation is nonlinear, $\bar{R}_{\mu\nu}$ is in general not linear in $h_{\mu\nu}$. The linear term in Eq. (C1) must obey the vacuum equation,

$$R^{(1)}_{\mu\nu} = 0. \qquad (C2)$$

This is an equation for the propagation of the gravitational waves, which corresponds to Eq. (9) or more generally to Eq. (D23) in the Friedman-Robertson-Walker (FRW) universe. The remaining part of $R_{\mu\nu}$ may be divided into a smooth part which varies only on scales larger than some coarse-graining scales,

$$\bar{R}_{\mu\nu} + \langle R^{(2)}_{\mu\nu} \rangle = 0, \qquad (C3)$$

and a fluctuating part which varies on smaller scales

$$R^{(1)\text{nonlinear}}_{\mu\nu} + R^{(2)}_{\mu\nu} - \langle R^{(2)}_{\mu\nu} \rangle = 0, \qquad (C4)$$

up to the second order in $h_{\mu\nu}$. Here, $R^{(1)\text{nonlinear}}_{\mu\nu}$ is defined by Eq. (C4) and represents the nonlinear correction to the propagation of $h_{\mu\nu}$, Eq. (C2), which gives $h_{\mu\nu} \rightarrow h_{\mu\nu} + j_{\mu\nu}$, where $j_{\mu\nu} \sim \mathcal{O}(h^2)$ [46]. Equation (C3) represents how the stress energy in the gravitational waves creates the background curvature. The Einstein equation in vacuum is then

$$\bar{G}_{\mu\nu} = \bar{R}_{\mu\nu} - \frac{1}{2}\bar{R}\bar{g}_{\mu\nu} = 8\pi G T^{(\text{GW})}_{\mu\nu}, \qquad (C5)$$

$$T^{(\text{GW})}_{\mu\nu} \equiv -\frac{1}{8\pi G}\left(\langle R^{(2)}_{\mu\nu} \rangle - \frac{1}{2}\bar{g}_{\mu\nu}\langle R^{(2)} \rangle \right), \qquad (C6)$$

where $T^{(\text{GW})}_{\mu\nu}$ is a definition of the energy-momentum tensor for the gravitational waves and $\langle \ \rangle$ denotes an average over several wavelengths. The importance of the effective energy-momentum tensor is that it tells us how *backreaction* from energy density of gravitational waves would affect the expansion law of the background universe. Note that the *effective* energy-momentum tensor defined by Eq. (C6) is different from that defined by the Neother current of the Lagrangian density, $T^{\text{Neother}}_{\mu\nu} \equiv \frac{2}{\sqrt{-g}}\frac{\delta S^{(2)}}{\delta g^{\mu\nu}}$,

where $S^{(2)}$ is the second order perturbation in the Einstein-Hilbert action. These definitions coincide only deep inside the horizon. Note also that in the notation of [46], $G = 1$, but in our notation, $\hbar = c = 1$, $G = m^{-2}_{\text{Pl}}$, where m_{Pl} is the Plank mass. Since $\langle R^{(2)} \rangle = 0$ [46],

$$T^{(\text{GW})}_{\mu\nu} = \frac{1}{32\pi G}\langle h_{\alpha\beta|\mu} h^{\alpha\beta}{}_{|\nu} \rangle$$

$$= \frac{1}{32\pi G}\langle h_{\alpha\beta,\mu} h^{\alpha\beta}{}_{,\nu} \rangle + \mathcal{O}(h^3), \qquad (C7)$$

where $|$ is the covariant derivative with respective to background metric, $\bar{g}_{\mu\nu}$. Note that we have employed the TT gauge. In linear theory we neglect higher order terms in the energy-momentum tensor.

The energy density of gravitational waves, ρ_h, is defined by the 0-0 component of the energy-momentum tensor.

$$\rho_h(\tau) \equiv T^{(\text{GW})}_{00} = \frac{1}{32\pi G}\langle \dot{h}_{ij} \dot{h}^{ij} \rangle, \qquad (C8)$$

where h_{ij} is in the TT gauge. There are only two independent modes for gravitational waves;

$$h_{ij} = \begin{pmatrix} h_+ & h_\times & 0 \\ h_\times & -h_+ & 0 \\ 0 & 0 & 0 \end{pmatrix}, \qquad (C9)$$

where $+$ and $\times$ denote two independent polarization modes and their propagation direction is taken in $\hat{z}$ direction. Hence,

$$\rho_h(\tau) = \frac{2}{32\pi G}\langle \dot{h}^2_+ + \dot{h}^2_\times \rangle = \frac{1}{16\pi G a^2}\langle h'^2_+ + h'^2_\times \rangle$$

$$= \frac{1}{16\pi G a^2} \int \frac{d^3k}{(2\pi)^3} \int \frac{d^3k'}{(2\pi)^3} \langle (h'_{+,\mathbf{k}} h'_{+,\mathbf{k}'}$$

$$+ h'_{\times,\mathbf{k}} h'_{\times,\mathbf{k}'}) e^{i(\mathbf{k}+\mathbf{k}')\cdot\mathbf{x}} \rangle, \qquad (C10)$$

where Fourier transformation was done and $h^*_{\lambda,\mathbf{k}} = h_{\lambda,-\mathbf{k}}$ in the last step. For stochastic modes, the spatial average over several wavelengths, $\langle \ \rangle$, is equivalent to the ensemble average in $\mathbf{k}$-space;

$$\langle h'_{\lambda,\mathbf{k}} h'_{\lambda',\mathbf{k}'} \rangle = (2\pi)^3 \delta_{\lambda,\lambda'} \delta^{(3)}(\mathbf{k} + \mathbf{k}')|h'_{\lambda,k}|^2, \qquad (C11)$$

where $\lambda = +, \times$. Using (C10) and (C11), we obtain

$$\rho_h(\tau) = \frac{1}{16\pi G a^2} \int \frac{d^3k}{(2\pi)^3}[|h'_{+,k}(\tau)|^2 + |h'_{\times,k}(\tau)|^2]. \qquad (C12)$$

It is reasonable to assume that the primordial gravitational waves are unpolarized, i.e. $|h_{+,k}|^2 = |h_{\times,k}|^2$. Whenever we express the time evolution of some quantities, it is convenient to express them in terms of the transfer function, $\mathcal{T}(k\tau)$, and the primordial amplitude, $\Delta^2_{h,\text{prim}}$, defined as (12);

$$\rho_h(\tau) = \frac{1}{32\pi G a^2} \int d \ln k \Delta_{h,\mathrm{prim}}^2 [\mathcal{T}'(k\tau)]^2, \qquad \text{(C13)}$$

where

$$\Delta_{h,\mathrm{prim}}^2 \equiv 4 \frac{k^3}{2\pi^2} |h_k^{\mathrm{prim}}|^2 = \frac{16}{\pi} \left(\frac{H_{\mathrm{inf}}}{m_{Pl}} \right)^2. \qquad \text{(C14)}$$

Here, $|h_k^{\mathrm{prim}}|^2$ is the amplitude of gravitational waves outside the horizon, $|k\tau| \ll 1$, during inflation. Well inside the horizon averaging over several periods, the leading term of $\overline{[\mathcal{T}'(k\tau)]^2}$ is proportional to $\tau^{-2} \propto a^{-2}$ during the radiation era and $\propto \tau^{-4} \propto a^{-2}$ during the matter era. Thus $\rho_h \propto a^{-4}$, which is consistent with the fact that graviton is massless and thus relativistic.

It is common to define the relative spectral density as the normalized energy density per logarithmic scale.

$$\Omega_h(\tau, k) \equiv \frac{\tilde{\rho}_h(\tau, k)}{\rho_{\mathrm{cr}}(\tau)}, \qquad \tilde{\rho}_h(\tau, k) \equiv \frac{d\rho_h(\tau)}{d \ln k}, \qquad \text{(C15)}$$

where $\rho_{\mathrm{cr}}(\tau)$ is critical density of the universe, and $\tilde{\rho}_h(\tau, k)$ denotes energy density of the gravitational waves per logarithmic scale. Inserting (C13) into (C15), we obtain

$$\Omega_h(\tau, k) = \frac{\Delta_{h,\mathrm{prim}}^2}{32\pi G a^2 \rho_c(\tau)} [\mathcal{T}'(\tau, k)]^2. \qquad \text{(C16)}$$

Recalling Friedman equation, $H^2 = 8\pi G \rho_c/3$, (C16) becomes

$$\Omega_h(\tau, k) = \frac{\Delta_{h,\mathrm{prim}}^2}{12 H^2(\tau) a^2} [\mathcal{T}'(\tau, k)]^2. \qquad \text{(C17)}$$

In this paper, we shall evaluate this quantity exactly within the SM of elementary particles. For an analytical model, $\mathcal{T}'(\tau, k)$ is given by Eqs. (B11)–(B13).

APPENDIX D: COLLISIONLESS DAMPING DUE TO NEUTRINO FREE-STREAMING

In this Appendix, we review the effect of collisionless particles on gravitational waves. Treating relativistic neutrino gas by classical kinetic theory, the linearized Einstein-Boltzmann equation (5) can be written as an integro-differential equation (D23). The derivation of this integro-differential equation is given in the literature, for instance [16–18,30] for both scalar and tensor modes, [31] for scalar modes, and will be reviewed briefly in this Appendix.

At the temperature of ~ 2 MeV, where neutrinos decoupled and became out of equilibrium with photons, electrons, or positrons, the number of effective relativistic species is $g_*(\sim 2 \text{ MeV}) = 10.75$.[2] The free-streaming neutrino gas after their decoupling satisfies the collisionless Boltzmann equation, i.e. the Vlasov equation,

$$\frac{dF(x, P)}{dt} = 0, \qquad \text{(D1)}$$

where $F(x, P) = \bar{F}(P) + \delta F(x, P)$ is a distribution function. The distribution function of relativistic neutrinos is given by

$$\bar{F}(P^0) = \frac{g_\nu}{e^{P^0/T} + 1}, \qquad \text{(D2)}$$

where g_ν denotes the number of helicity states for neutrinos and antineutrinos. Here, $P^\mu \equiv \frac{dx^\mu}{d\lambda}$ and $P^0 = \sqrt{g_{ij} P^i P^j}$, which is implied by the constraint for relativistic particles;

$$g_{\mu\nu} P^\mu P^\nu = 0. \qquad \text{(D3)}$$

Therefore, there are only three independent components of the momentum vector. One can also relate P^i with $P_0 = -P^0$ as

$$P^i = \pm \frac{\gamma^i P_0}{a} \left(1 - \frac{1}{2} h_{jk} \gamma^j \gamma^k \right), \qquad \text{(D4)}$$

where $\gamma^i = \gamma_i$'s are directional cosines and P^0 is the energy of neutrinos. We chose positive sign convention for $P^0 \equiv \frac{dt}{d\lambda}$. Note that $\delta_{ij} \gamma^i \gamma^j = 1$, and $P^i \equiv C\gamma^i P_0$, where the coefficient, C, is obtained from Eq. (D3);

$$0 = P_0 P^0 + a^2 P^j P^j + a^2 h_{ij} P^i P^j,$$
$$0 = -(P_0)^2 + a^2 C^2 P_0^2 + a^2 h_{ij} \gamma^i \gamma^j C^2 P_0^2,$$
$$1 = a^2 C^2 (1 + h_{ij} \gamma^i \gamma^j).$$

We consider tensor perturbations. Equation (D1) can be expressed as

$$\frac{dF(t, x^i, \gamma^i, P^0)}{dt} = \frac{\partial F}{\partial t} + \frac{dx^i}{dt} \frac{\partial F}{\partial x^i} + \frac{dP^0}{dt} \frac{\partial F}{\partial P^0} + \frac{d\gamma^i}{dt} \frac{\partial F}{\partial \gamma^i}$$
$$= 0. \qquad \text{(D5)}$$

The last term is negligible in the linear perturbation theory, as $\frac{\partial F}{\partial \gamma^i}$ is of the first order in perturbations and $\dot{\gamma}^i = -\frac{1}{2a} h_{jk,i} \gamma^j \gamma^k$.

For the second term $\frac{\partial F}{\partial x^i}$ is of the first order in perturbations and

$$\frac{dx^i}{dt} = \frac{dx^i}{d\lambda} \frac{d\lambda}{dt} = \frac{P^i}{P^0}. \qquad \text{(D6)}$$

Using Eq. (D4), one obtains

$$\frac{dx^i}{dt} \frac{\partial F}{\partial x^i} = \frac{\gamma^i}{a} \frac{\partial F}{\partial x^i} \qquad \text{(D7)}$$

in the leading order, as $\bar{F}$ does not depend on x^i; thus, $\frac{\partial F}{\partial x^i}$ is a perturbation.

For the third term we use the geodesic equation,

$$\frac{dP^\mu}{d\lambda} = -\Gamma^\mu{}_{\alpha\beta} P^\alpha P^\beta, \qquad \text{(D8)}$$

---

[2]We have assumed instantaneous decoupling of neutrinos, but this is not true in general.

$$\Gamma^\mu_{\ \alpha\beta} = \frac{g^{\mu\nu}}{2}\left[\frac{\partial g_{\alpha\nu}}{\partial x^\beta} + \frac{\partial g_{\beta\nu}}{\partial x^\alpha} - \frac{\partial g_{\alpha\beta}}{\partial x^\nu}\right]. \qquad \text{(D9)}$$

The time component of the geodesic equation is

$$\begin{aligned}\frac{dt}{d\lambda}\frac{dP^0}{dt} &= -\Gamma^0_{\ \alpha\beta}P^\alpha P^\beta,\\ &= -\frac{g^{0\nu}}{2}\left[2\frac{\partial g_{\alpha\nu}}{\partial x^\beta} - \frac{\partial g_{\alpha\beta}}{\partial x^\nu}\right]P^\alpha P^\beta, \qquad \text{(D10)}\\ &= -\frac{\dot a}{a}(P^0)^2 - \frac{1}{2}a^2\frac{\partial h_{ij}}{\partial t}P^i P^j,\end{aligned}$$

where $g_{00} = -1$, $g_{0i} = 0$ were used from the second line to the last line. Up to the first order in perturbations

$$\frac{1}{P^0}\frac{dP^0}{dt} = -\frac{\dot a}{a} - \frac{1}{2}\frac{\partial h_{ij}}{\partial t}\gamma^i\gamma^j, \qquad \text{(D11)}$$

where we have used Eq. (D4) and neglected higher order terms. This equation describes the change in the neutrino energy as it propagates in a FRW universe with gravitational waves. The first term accounts for the redshift of energy due to an isotropic expansion. The second term tells us that neutrinos lose energy if $\frac{\partial h_{ij}}{\partial t} > 0$, or gain energy if $\frac{\partial h_{ij}}{\partial t} < 0$ from gravitational waves. This energy flow from neutrinos to gravitational waves causes collisionless damping (Figs. 8 and 9) and amplification (Fig. 10) of gravitational waves.
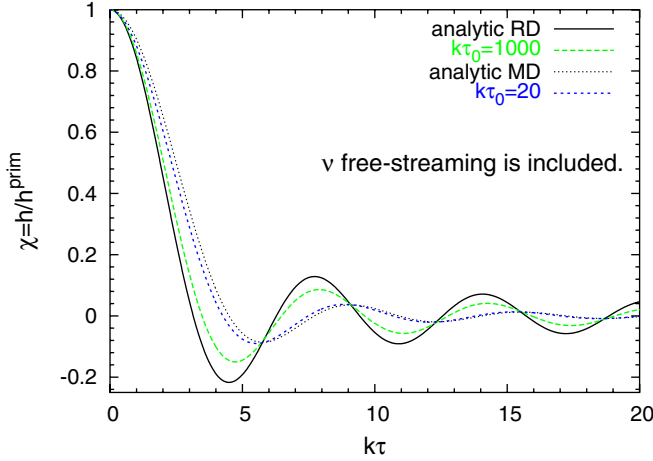

FIG. 8 (color online). Comparison between numerical solutions and analytical solutions of tensor perturbations. The effect of neutrino free-streaming is included for numerical solutions, but not for analytical solutions. The dashed and short-dashed lines show numerical solutions of the high and low frequency modes, respectively. The higher k-modes enter the horizon during the radiation era after neutrino decoupling, and thus the numerical solution is damped by neutrino free-streaming compared to the analytical solution, $\chi(k\tau) = j_0(k\tau)$ (solid line). On the other hand, the lower k-modes enter the horizon much later, and thus the numerical solution is closer to the analytical solution during the matter era, $\chi(k\tau) = 3j_1(k\tau)/k\tau$ (dotted line).
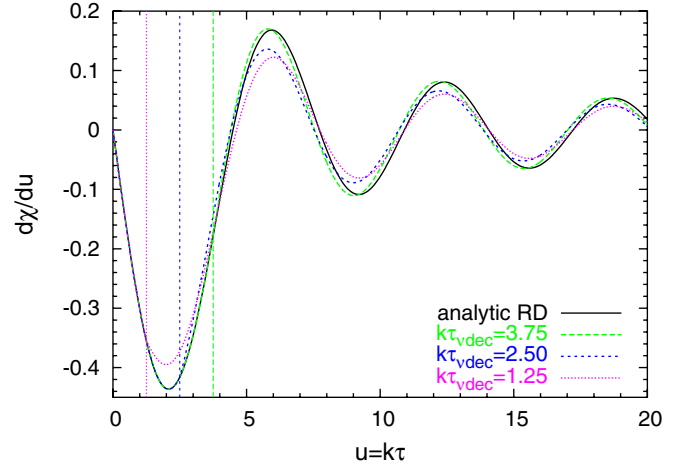

FIG. 9 (color online). Derivatives of modes which entered the horizon before neutrino decoupling. The solid line shows an analytical solution, $\chi' = -j_1(u)$, during the radiation era without neutrino decoupling. The dotted, short-dashed, and dashed lines show numerical solutions of $\chi'(k\tau)$ for which neutrinos decoupled at $\tau_{\nu\,\text{dec}}$ given by $k\tau_{\nu\,\text{dec}} = 1.25$, 2.5, 3.75, respectively. They are damped by giving energy to free-streaming neutrinos. Vertical lines indicate the neutrino decoupling time for each mode.

Finally, by combining Eqs. (D5), (D7), and (D11), the Vlasov equation for the first order perturbations is obtained as

$$\begin{aligned}\left(\frac{dF}{dt}\right)_{\text{first order}} &= \frac{\partial\delta F}{\partial t} + \frac{\gamma^i}{a}\frac{\partial\delta F}{\partial x^i} - P^0\frac{\partial\delta F}{\partial P^0}\frac{\dot a}{a} - P^0\frac{\partial\bar F}{\partial P^0}\frac{1}{2}\\ &\quad \times\frac{\partial h_{ij}}{\partial t}\gamma^i\gamma^j = 0, \qquad \text{(D12)}\end{aligned}$$
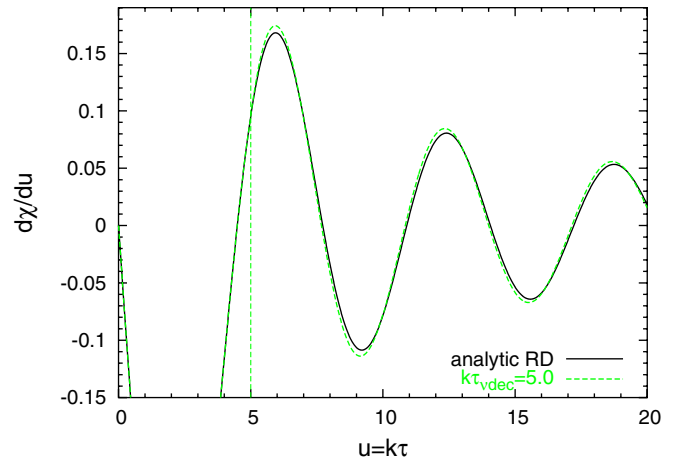

FIG. 10 (color online). Derivative of a mode which entered the horizon before neutrino decoupling. The solid line shows an analytic solution, $\chi' = -j_1(u)$, during the radiation era without neutrino decoupling. The dashed line shows numerical solutions of $\chi'(k\tau)$ for which neutrinos decoupled at $\tau_{\nu\,\text{dec}}$ given by $k\tau_{\nu\,\text{dec}} = 5.0$. The wave is amplified by gaining energy from free-streaming neutrinos. The vertical line indicates the neutrino decoupling time.

where $F = \bar{F} + \delta F(t, x^i, \gamma^i, P^0)$ and δF is a tensor type perturbation in a distribution function of neutrinos. The zeroth order Vlasov equation merely gives cosmological redshift, $P^0 \propto a^{-1}$, as explained above. Defining $\mu \equiv \gamma^i k_i / k$ and Fourier transforming Eq. (D12), the first order Vlasov equation in the momentum space is given as

$$\frac{\partial f_k}{\partial t} - \frac{\dot{a}}{a} P^0 \frac{\partial f_k}{\partial P^0} + \frac{ik\mu}{a} f_k = P^0 \frac{\partial \bar{F}}{\partial P^0} \frac{1}{2} \frac{\partial h_k}{\partial t}, \quad (D13)$$

where we have used

$$h_{ij}(t, \mathbf{x}) = \sum_{\lambda=+,\times} \int \frac{d^3k}{(2\pi)^3} h_{\lambda,k}(t) Q_{ij}^{\lambda}(\mathbf{x}), \quad (D14)$$

$$\delta F = \sum_{\lambda=+,\times} \int \frac{d^3k}{(2\pi)^3} f_{\lambda,k}(t, P^0, \mu) \gamma^i \gamma^j Q_{ij}^{\lambda}(\mathbf{x}). \quad (D15)$$

Here, tensor harmonics $Q_{ij}^{\lambda}(\mathbf{x})$ are solutions of the tensor Helmholtz equation; $Q_{ij|a}^{\lambda}{}^a(\mathbf{x}) + k^2 Q_{ij}^{\lambda}(\mathbf{x}) = 0$, $\partial_l Q_{ij}^{\lambda} = ik_l Q_{ij}^{\lambda}$. They are symmetric, traceless, and divergenceless; $Q_{ij}^{\lambda} = Q_{ji}^{\lambda}$, $\gamma^{ij} Q_{ij}^{\lambda} = Q_{ij}^{\lambda} = 0$, where $\gamma^{ij} \equiv a^2 \bar{g}^{ij}$ and $|$ denotes the covariant derivative with respect to the spatial metric γ^{ij}. Note that Fourier transformation here is the generalization of Eq. (4) for arbitrary spatial geometry of the universe. One can treat $Q_{ij}^{\lambda}(\mathbf{x})$ as a plane wave in a flat geometry case.

Because of the existence of the second term on the left-hand side of Eq. (D13), we cannot solve this equation. Thus following [31], we introduce the comoving momentum, $q^\mu \equiv aP^\mu$. Regarding F as a function of comoving energy, $q \equiv q^0$, and conformal time, τ, the third term in Eq. (D5) may be replaced by $\frac{dq}{d\tau} \frac{\partial F}{\partial q} = -\frac{1}{2} q h'_{ij} \gamma^i \gamma^j \frac{\partial \bar{F}}{\partial q}$ up to the linear order. Then the linearized Vlasov equation, $\frac{d}{d\tau} F(\tau, x^i, \gamma^i, q) = 0$, becomes

$$\frac{\partial f_k}{\partial \tau} + ik\mu f_k = q \frac{\partial \bar{F}}{\partial q} \frac{1}{2} \frac{\partial h_k}{\partial \tau}, \quad (D16)$$

where $f_k = f_k(\tau, q, \mu)$. One finds the solution of Eq. (D16) as

$$f_k(\tau, q, \mu) = e^{-i\mu k(\tau - \tau_{\nu \text{ dec}})} f_k(\tau_{\nu \text{ dec}}, q, \mu) + \frac{q}{2} \frac{\partial \bar{F}}{\partial q}$$
$$\times \int_{\tau_{\nu \text{ dec}}}^{\tau} d\tau' h'_k(\tau') e^{-i\mu k(\tau - \tau')}, \quad (D17)$$

where the prime on $h_k(\tau)$ denotes the derivative with respect to the conformal time. As there is no primordial tensor perturbations in the neutrino distribution function before neutrino decoupling, $f_k(\tau_{\nu \text{ dec}}, q, \mu) = 0$.

The right-hand side of the linearized Einstein equation includes anisotropic stress as in Eq. (5);

$$\delta T_{ij}^{(\nu)} = a^2 \sum_{\lambda=+,\times} \int \frac{d^3k}{(2\pi)^3} \Pi_{\lambda,k} Q_{ij}^{\lambda}(\mathbf{x}), \quad (D18)$$

where $T_{ij}^{(\nu)}$ denotes the stress-energy tensor of neutrinos. Since $T_{ij}^{(\nu)} = \frac{1}{\sqrt{-g}} \int \frac{d^3q}{q^0} q_i q_j F(q)$, its perturbation can be expressed as

$$\delta T_{ij}^{(\nu)} = a^{-4} \int \frac{d^3q}{q^0} [\bar{q}_i \bar{q}_j \delta F + (\delta q_i \bar{q}_j + \bar{q}_i \delta q_j) \bar{F}],$$
$$\delta F = \sum_{\lambda=+,\times} \int \frac{d^3k}{(2\pi)^3} f_{\lambda,k}(\tau, q, \mu) \gamma^l \gamma^m Q_{lm}^{\lambda}(\mathbf{x}). \quad (D19)$$

The second and the third terms of (D19) cancel out in linear perturbation theory. Thus

$$\Pi_{\lambda,k} Q_{ij}^{\lambda}(\mathbf{x}) = a^{-4} \int \frac{d^3q}{q^0} q^2 \gamma^i \gamma^j \gamma^l \gamma^m f_{\lambda,k} Q_{lm}^{\lambda}(\mathbf{x}). \quad (D20)$$

Inserting solution of the Vlasov Eq. (D17) into Eq. (D20) and using equality $\int d\Omega_q \gamma^i \gamma^j \gamma^l \gamma^m e^{-i\hat{\gamma} \cdot \hat{k}u} Q_{lm}^{\lambda} = \frac{1}{8} \times (\delta^{il} \delta^{jm} + \delta^{im} \delta^{jl}) \int d\Omega_q e^{-i\mu u} (1 - 2\mu^2 + \mu^4) Q_{lm}^{\lambda}$, one obtains

$$\Pi_k = \frac{1}{4a^4} \int d^3q q (1 - 2\mu^2 + \mu^4) f_k,$$
$$= -4\bar{\rho}_\nu(\tau) \int_{\tau_{\nu \text{ dec}}}^{\tau} d\tau' \left(\frac{j_2[k(\tau - \tau')]}{k^2(\tau - \tau')^2} \right) h'_k(\tau'). \quad (D21)$$

Here, $\bar{q}_i = aq\gamma^i$ and $\bar{q}^i = a^{-1}q\gamma^i$, and $\bar{\rho}_\nu(\tau) = a^{-4} \int d^3q q \bar{F}(q)$ is the unperturbed neutrino energy density, and a negative sign appears on the right-hand side of Eq. (D21) because integration by parts has been done. Also, we have used the identity

$$\frac{1}{16} \int_{-1}^{1} d\mu (1 - 2\mu^2 + \mu^4) e^{-i\mu u} = \frac{j_2(u)}{u^2}. \quad (D22)$$

Note that $\frac{j_2(-u)}{(-u)^2} = \frac{j_2(u)}{u^2}$, $\int_{-\infty}^{\infty} \frac{j_2(u)}{u^2} du = \frac{\pi}{8}$, and $\lim_{u \to 0} \frac{j_2(u)}{u^2} = \frac{1}{15}$.[3]

Then the Einstein-Vlasov equation takes a form of an integro-differential equation;

$$h_k''(\tau) + \left[\frac{2a'(\tau)}{a(\tau)} \right] h_k'(\tau) + k^2 h_k(\tau)$$
$$= -24 f_\nu(\tau) \left[\frac{a'(\tau)}{a(\tau)} \right]^2 \int_{\tau_{\nu \text{ dec}}}^{\tau} d\tau' \left[\frac{j_2[k(\tau - \tau')]}{k^2(\tau - \tau')^2} \right] h_k'(\tau'), \quad (D23)$$

and the fraction of the total energy density in neutrinos is

$$f_\nu(\tau) \equiv \frac{\bar{\rho}_\nu(\tau)}{\bar{\rho}(\tau)} = \frac{\Omega_\nu (a_0/a)^4}{\Omega_M (a_0/a)^3 + (\Omega_\gamma + \Omega_\nu)(a_0/a)^4}$$
$$= \frac{f_\nu(0)}{1 + a(\tau)/a_{\text{EQ}}}, \quad (D24)$$

---

[3]In the Refs. [18,33], $K[u] \equiv -\frac{\sin u}{u^3} - \frac{3 \cos u}{u^4} + \frac{3 \sin u}{u^5} = \frac{1}{15}(j_0(u) + \frac{10}{7} j_2(u) + \frac{3}{7} j_4(u))$, which is the same function as our kernel, i.e. $K[u] = \frac{j_2(u)}{u^2}$.

where

$$f_\nu(0) = \frac{\Omega_\nu}{\Omega_\gamma + \Omega_\nu} = 0.40523. \quad \text{(D25)}$$

The integro-differential Eq. (D23) was studied in [18,32–34] in the cosmological context. Here we shall solve this equation numerically with all the SM particles participating in the cosmic thermal plasma. Anisotropic stress, Π_k, vanishes during the matter era, as $f_\nu \to 0$. Therefore, the damping effect is unimportant during the matter era.

Following [18], we write

$$h_\lambda(u) \equiv h_\lambda(0)\chi(u), \quad \text{(D26)}$$

which gives

$$\chi''(u) + \left[\frac{2a'(u)}{a}\right]\chi'(u) + \chi(u)$$
$$= -24 f_\nu(u)\left[\frac{a'(u)}{a}\right]^2 \int_{u_{\nu\,\text{dec}}}^u dU \left[\frac{j_2(u-U)}{(u-U)^2}\right]\chi'(U),$$
$$\text{(D27)}$$

where $u \equiv k\tau$, and derivatives are taken with respect to u. After the end of inflation, τ_{end}, the amplitude of cosmological fluctuations is conserved until the mode re-enter the horizon, $h_\lambda(0) = h_{\lambda,\mathbf{k}}(\tau_{\text{end}})$. Note that the right-hand side of Eq. (D27) disappears on the superhorizon scales—neutrino free-streaming affects the tensor metric perturbation only inside the horizon. The initial conditions are taken to be

$$\chi(0) = 1, \qquad \chi'(0) = 0. \quad \text{(D28)}$$

We solve Eq. (D27) numerically by two steps; (i) we obtain $a(\tau)$ and $a'(\tau)$ from the Friedman equation (26) with $g_*(\tau)$ in Sec. III [Fig. 3], and (ii) we solve Eq. (D27) with the scale factor that we obtained in the step (i) The numerical solutions as well as analytical solutions are presented and compared in Fig. 8. The higher Fourier modes enter the horizon during the radiation era, but after neutrino decoupling. Thus they are damped due to the presence of the right-hand side of Eq. (D27).

In order to estimate the damping effect, let us consider the radiation era after neutrino decoupling. During the radiation era, $a'(u)/a = 1/u$, the analytical solution is given by $\chi(u) = j_0(u)$ in the absence of neutrino free-streaming in Eq. (D27). In the presence of neutrino free-streaming, the solution becomes asymptotically ($u \gg 1$)

$$\chi(u) \to A \frac{\sin(u+\delta)}{u}, \quad \text{(D29)}$$

where $A = 0.80313$ and $\delta = 0$ are obtained from our numerical calculations. This asymptotic solution is valid only for rather long wavelength modes which entered the horizon well after the neutrino decoupling. The suppression factor $A^2 = 0.64502$ applies to the gravitational wave spectrum of the modes that entered the horizon after neutrino decoupling but before matter domination.

In order to understand the shape of the spectrum, Figs. 4 and 5, we need to consider shorter wavelength modes as well. This may be understood as follows. As we saw in Eq. (D11), if the time derivative of the mode is negative (positive), the mode is damped (amplified). Integrating the amplitude of gravitational waves over time, the net effect of neutrino free-streaming almost always damps gravitational waves. This is because the contribution is mainly from the first period of $\chi'(u)$, where the first trough is larger than the first peak. In previous paragraph we have considered the modes with $k\tau_{\nu\,\text{dec}} < 1$. Now let us consider the higher k-modes with $k\tau_{\nu\,\text{dec}} \sim 1$, or $k \sim 10^{-10}$–10^{-9} Hz. Note that $k\tau_{\nu\,\text{dec}} = 1$ represents the mode which entered the horizon at the neutrino decoupling time, $\tau_{\nu\,\text{dec}}$. The mode with larger wavenumbers would enter the horizon earlier. Figure 9 shows numerical solutions of $\chi'(u)$ for which neutrinos decoupled at $\tau_{\nu\,\text{dec}}$ given by $k\tau_{\nu\,\text{dec}} = 1.25$, 2.5, or 3.75. For $k\tau_{\nu\,\text{dec}} = 1.25$ and 2.5, neutrinos decoupled at the first trough of $\chi'(u)$, where $\chi'(u)$ is negative. Thus their amplitudes are damped by giving energy to free-streaming neutrinos (see Eq. (D11) and discussion below it). For $k\tau_{\nu\,\text{dec}} = 3.75$, neutrinos decoupled right after the first trough of $\chi'(u)$, where $\chi'(u)$ is closer to zero. Thus its amplitude is unchanged, but its phase is delayed. Figure 10 shows numerical solutions of $\chi'(u)$ with $k\tau_{\nu\,\text{dec}} = 5.0$. For $k\tau_{\nu\,\text{dec}} = 5.0$, neutrinos decoupled at the first peak of $\chi'(u)$, where $\chi'(u)$ is positive. Thus the amplitude of gravitational waves is actually amplified by gaining energy from free-streaming neutrinos, and we can see this feature on the spectrum, Fig. 5, at $\sim 5 \times 10^{-10}$ Hz. Neutrino free-streaming makes gravitational waves either damp or amplify depending on their frequencies. Note that this feature is generic to instantaneous decoupling of any kinds of particles, but not realistic for neutrinos as we mentioned in Sec. IV.

For extremely short wavelength modes which have already been inside the horizon before neutrino decoupling, $k\tau_{\nu\,\text{dec}} \gg 1$ or $k > 10^{-9}$ Hz, the suppression becomes negligibly small; $A \to 1$, but the phase delay, δ, is nonzero. These modes are undamped as positive and negative contributions of χ' to the gravitational wave energy cancel out each other after several periods of χ'. No net energy conversion from gravitational waves to free-streaming neutrinos would occur.

APPENDIX E: OSCILLATION DUE TO DRASTIC CHANGE OF $g_*(\tau)$

In this Appendix we explain the effect on the gravitational wave spectrum from a sudden change in the number of relativistic species, g_*. To do this, we need to calculate $\Omega_h^{\text{out}}(k_2)/\Omega_h^{\text{in}}(k_1)$, where $k_2 \neq k_1$. In Sec. IV we have already seen the numerical prediction of the gravitational wave spectrum. In subsection III B we provided the way to

understand the relative suppression of gravitational waves at a given k ($= k_1 = k_2$) with and without changes in g_*. We shall discuss in a similar way what would happen to different Fourier modes, in order to fully understand imprints of g_* on the spectrum, such as oscillations, which are from cosmological events that change g_* instantaneously or drastically.

In Fig. 5 we find an oscillatory feature at around 10^{-7} Hz, which corresponds to the mode entering the horizon at the QGP phase transition. At this energy scale, ~ 180 MeV, the effective number of relativistic species changes drastically, giving a sharp feature and oscillation in Ω_h. To understand this, let us consider the simple analytical model employed in subsection III B. Equation (40) is the mode which experienced such a change of g_* and its coefficients A, B, C and D are

$$A(s, n) = \frac{\pi}{4s^{3/2}}\big[-2sY_{1+\sqrt{1+4n}/2}(s)\sin s + Y_{\sqrt{1+4n}/2}(s)$$
$$\times (-2s\cos s + (3 + \sqrt{1+4n})\sin s)\big], \quad (E1)$$

$$B(s, n) = -\frac{\pi}{4s^{3/2}}\big[-2sJ_{1+\sqrt{1+4n}/2}(s)\sin s + J_{\sqrt{1+4n}/2}(s)$$
$$\times (-2s\cos s + (3 + \sqrt{1+4n})\sin s)\big], \quad (E2)$$

$$C(s, t, n) = \frac{\pi}{4\sqrt{st}}\sec n\pi\big[-2tJ_{-n-3/2}(t)\cos t(J_{n+1/2}(s)$$
$$\times (s\cos s - \sin s) + sJ_{n+3/2}(s)\sin s)$$
$$- 2J_{-n-1/2}(t)(J_{n+1/2}(s)(s\cos s - \sin s)$$
$$+ sJ_{n+3/2}(s)\sin s)(\cos t + t\sin t)$$
$$+ 2(J_{-n-1/2}(s)(s\cos s - \sin s)$$
$$- sJ_{-n-3/2}(s)\sin s)(-tJ_{n+3/2}(t)$$
$$\times \cos t + J_{n+1/2}(t)(\cos t + t\sin t))\big], \quad (E3)$$

$$D(s, t, n) = \frac{\pi}{4\sqrt{st}}\sec n\pi\big[2tJ_{n+1/2}(t)\cos t(J_{-n-1/2}(s)$$
$$\times (-s\cos s + \sin s) + sJ_{-n-3/2}(s)\sin s)$$
$$- 2J_{-n-1/2}(t)(J_{n+1/2}(s)(s\cos s - \sin s)$$
$$+ sJ_{n+3/2}(s)\sin s)(t\cos t - \sin t)$$
$$- 2\sin t(tJ_{-n-3/2}(t)(J_{n+1/2}(s)(s\cos s - \sin s)$$
$$+ sJ_{n+3/2}(s)\sin s) + (-tJ_{n+3/2}(t)$$
$$\times \cos t + J_{n+1/2}(t))(sJ_{-n-3/2}(s)\sin s$$
$$+ J_{-n-1/2}(s)(-s\cos s + \sin s)))\big], \quad (E4)$$

where $s \equiv k\tau_2$, $t \equiv k\tau_1$ and $s \leq t$. Here, $J_n(x)$ and $Y_n(x)$
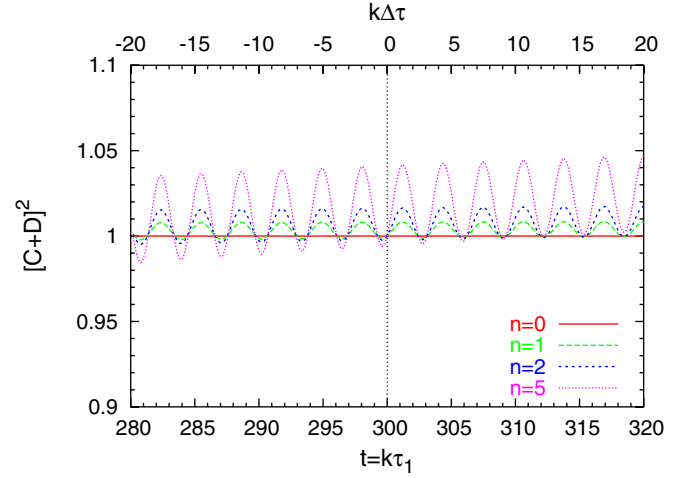

FIG. 11 (color online). The oscillatory factor $[C + D]^2$ with respect to $t \equiv k\tau_1$. The vertical line indicates $s \equiv k\tau_2 = 300 \leq t$ and $\Delta\tau \equiv \tau_1 - \tau_2 = 0$. The solid, dashed, short-dashed, and dotted lines show $n = 0$, 1, 2, and 5, respectively. The factor, $[C + D]^2$, takes on unity at $\Delta\tau \to 0$ regardless of n.

are the Bessel function and Neumann function, respectively. At this time, we are interested in different k-modes, $k_1 < k_2$. (However we evaluate $\Omega_h(k)$ at the same time, τ.) We obtain

$$\frac{\Omega^{\mathrm{in}}(k_2)}{\Omega^{\mathrm{out}}(k_1)} \simeq \frac{k_2^2 h^2(k_2\tau)}{k_1^2 h^2(k_1\tau)},$$
$$= \left(\frac{k_2}{k_1}\right)^2 \left(\frac{\tau_2}{\tau_1}\right)^{2n} \left[C(k_2)\frac{j_0(k_2\tau)}{j_0(k_1\tau)} + D(k_2)\frac{y_0(k_2\tau)}{j_0(k_1\tau)}\right]^2,$$
$$\approx \left(\frac{k_2}{k_1}\right)^2 \left(\frac{\tau_2}{\tau_1}\right)^{2n} \left[C(k_2)\frac{k_1}{k_2} + D(k_2)\frac{k_1}{k_2}\right]^2,$$
$$= \left(\frac{\tau_2}{\tau_1}\right)^{2n}[C(k_2) + D(k_2)]^2 \to \left(\frac{\tau_2}{\tau_1}\right)^{2n} = \left(\frac{s}{t}\right)^{2n},$$
$$(E5)$$

where $\simeq$ denotes the subhorizon limit, $\approx$ denotes the asymptotic limit as $k\tau \to$ large, and $\to$ denotes the limit in $\Delta k \equiv k_2 - k_1 \to 0$. Equation (E5) tells us the exact ratio between different k-modes. While we obtained only the suppression factor, $(\tau_2/\tau_1)^{2n}$, in subsection III B, we now also obtain the oscillatory factor, $[C + D]^2$. Figure 11 shows that the factor, $[C + D]^2$, oscillates and takes on unity at $\Delta\tau \to 0$ regardless of n. Here, $n = 5$ represents $g_* \propto \tau^{-30}$, which is an extremely drastic change. This gives us a complete analytical account of the shape of Fig. 5.

[1] L. P. Grishchuk, Sov. Phys. JETP **40**, 409 (1975); Classical Quantum Gravity **10**, 2449 (1993).
[2] A. A. Starobinsky, JETP Lett. **30**, 682 (1979).
[3] V. A. Rubakov, M. V. Sazhin, and A. V. Veryaskin, Phys. Lett. B **115**, 189 (1982).
[4] R. Fabbri and M. D. Pollock, Phys. Lett. B **125**, 445 (1983).
[5] L. F. Abbott and M. B. Wise, Nucl. Phys. B **244**, 541 (1984).
[6] A. A. Starobinsky, Sov. Astron. Lett. **11**, 133 (1985).
[7] L. H. Ford, Phys. Rev. D **35**, 2955 (1987).
[8] B. Allen, Phys. Rev. D **37**, 2078 (1988).
[9] V. Sahni, Phys. Rev. D **42**, 453 (1990).
[10] M. S. Turner, M. White, and J. E. Lidsey, Phys. Rev. D **48**, 4613 (1993).
[11] M. White, Phys. Rev. D **46**, 4198 (1992).
[12] M. S. Turner, Phys. Rev. D **48**, 3502 (1993); Phys. Rev. D **55**, R435 (1997).
[13] M. Kamionkowski, A. Kosowsky, and M. S. Turner, Phys. Rev. D **49**, 2837 (1994).
[14] D. J. Schwarz, Mod. Phys. Lett. A **13**, 2771 (1998); Ann. Phys. (Berlin) **12**, 220 (2003).
[15] D. A. Dicus et al., Phys. Rev. D **26**, 2694 (1982).
[16] E. T. Vishniac, Astrophys. J. **257**, 456 (1982).
[17] A. K. Rebhan and D. J. Schwarz, Phys. Rev. D **50**, 2541 (1994).
[18] S. Weinberg, Phys. Rev. D **69**, 023503 (2004).
[19] A. H. Guth, Phys. Rev. D **23**, 347 (1981).
[20] A. D. Linde, Phys. Lett. B **108**, 389 (1982).
[21] A. Albrecht and P. J. Steinhardt, Phys. Rev. Lett. **48**, 1220 (1982).
[22] T. L. Smith, M. Kamionkowski, and A. Cooray, Phys. Rev. D **73**, 023504 (2006).
[23] T. L. Smith, H. W. Peris, and A. Cooray, astro-ph/0602137.
[24] J. Khoury, B. A. Ovrut, P. J. Steinhardt, and N. Turok, Phys. Rev. D **64**, 123522 (2001).
[25] S. Phinney et al., NASA Mission Concept Study, [http://universe.nasa.gov/program/bbo.html].
[26] N. Seto, S. Kawamura, and T. Nakamura, Phys. Rev. Lett. **87**, 221103 (2001).
[27] J. M. Bardeen, Phys. Rev. D **22**, 1882 (1980).
[28] H. Kodama and M. Sasaki, Prog. Theor. Phys. Suppl. **78**, 1 (1984).
[29] S. Weinberg, *Gravitation and Cosmology* (Wiley, New York, 1972).
[30] M. Kasai and K. Tomita, Phys. Rev. D **33**, 1576 (1986).
[31] J. R. Bond and A. S. Szalay, Astrophys. J. **274**, 443 (1983).
[32] J. R. Pritchard and M. Kamionkowski, Ann. Phys. (N.Y.) **318**, 2 (2005).
[33] D. A. Dicus and W. W. Repko, Phys. Rev. D **72**, 088302 (2005).
[34] S. Bashinsky, astro-ph/0505502.
[35] S. W. Hawking and W. Israel, *300 Years of Gravitation* (Cambridge University Press, Cambridge, 1987), pp. 330–458.
[36] E. W. Kolb and M. S. Turner, *The Early Universe* (Addison-Wesley, Reading, MA, 1990).
[37] G. Mangano et al., Phys. Lett. B **534**, 8 (2002).
[38] M. Hindmarsh and O. Philipsen, Phys. Rev. D **71**, 087302 (2005).
[39] M. Maggiore, Phys. Rep. **331**, 283 (2000).
[40] N. Seto and J. Yokoyama, J. Phys. Soc. Jpn. **72**, 3082 (2003).
[41] L. A. Boyle and P. J. Steinhardt, astro-ph/0512014.
[42] Y. Zhang et al., Classical Quantum Gravity **23**, 3783 (2006).
[43] N. D. Birrell and P. C. W. Davies, *Quantum Fields in Curved Space* (Cambridge University Press, Cambridge, 1982).
[44] D. N. Spergel et al., Astrophys. J. Suppl. Ser. **148**, 175 (2003).
[45] K. Ng and A. D. Speliotopoulos, Phys. Rev. D **52**, 2112 (1995); K. Ng, Int. J. Mod. Phys. A **11**, 3175 (1996).
[46] C. W. Misner, K. S. Thorne, and J. A. Wheeler, *Gravitation* (Freeman, NY, 1973).